Advances in Materials. Separations: Materials, Devices and Processes

Thermally Induced Phase Separation and Electrospinning Methods for Emerging Membrane Applications: A Review

Jeong F. Kim, Ji Hoon Kim, and Young Moo Lee
Dept. of Energy Engineering, Hanyang University, Seoul, Republic of Korea

Enrico Drioli
Dept. of Energy Engineering, Hanyang University, Seoul, Republic of Korea

National Research Council Institute on Membrane Technology (ITM-CNR), The University of Calabria, Rende, Cosenza, Italy

DOI 10.1002/aic.15076
Published online November 5, 2015 in Wiley Online Library (wileyonlinelibrary.com)

In this review, thermally induced phase separation (TIPS) and electrospinning methods for preparation of fluoropolymer membranes are assessed, particularly for the polyvinylidene fluoride (PVDF) and polyethylene chlorotrifluoroethylene membranes. This review focuses on controlling the membrane morphology from the thermodynamic and kinetic perspectives to understand the relationship between the membrane morphology and fabrication parameters. In addition, the current status of the nonsolvent induced phase separation (NIPS) method and the combined NIPS-TIPS (N-TIPS) method, which is a new emerging fabrication method, are discussed. The past literature data are compiled and an upperbound curve (permeability vs. tensile strength) is proposed for the TIPS-prepared PVDF membranes. Furthermore, the key parameters that control and determine the membrane morphology when using the electrospinning method are reviewed. Exploiting the unique advantages of the electrospinning method, our current understanding in controlling and fine-tuning the PVDF crystal polymorphism (i.e., β-phase) is critically assessed. © 2015 American Institute of Chemical Engineers *AIChE J*, 62: 461–490, 2016

Keywords: membrane materials, membrane separations, green engineering, fibers, polymer processing

Introduction: Current Membrane Technology Status

In the field of separation technology, the demands for improved processes are always high due to the needs to meet stricter quality requirements and environmental regulations without compromising the overall unit efficiency. A simple and innovative way to improve a process is to use a hybrid configuration combining two or more unit operations. In that sense, membranes are ideal for such hybrid processes due to their high modularity and flexible operation that can be integrated with many existing unit operations.

The core concept of membrane processes lies in the use of a membrane as a barrier to selectively transport solutes of interest. The driving force for separation may be a pressure gradient, temperature gradient, and/or concentration gradient. The separation mechanism could be due to the difference in solute sizes or solute interactions with the membrane, where the separation efficiency depends on many different parameters. Different types of membrane processes and typical solutes of interest are summarized in Figure 1.

Membrane technology is now a well-established technology in industrial processes with applications ranging from desalination[1] and wastewater treatment,[2] to biotechnology,[3] textile manufacturing,[4] gas separation,[5] and food processing.[6] The field of membrane technology is also growing rapidly. The new desalination plants coming online are mostly membrane-based, new wastewater treatment plants are increasingly adopting the membrane bioreactor (MBR) technology because of its high efficiency, and at least one or two membrane-based unit operations are typically used in dairies and breweries.[7]

Membrane technology, from the chemical engineering perspectives, has many unique advantages such as high modularity and easy integration into existing unit operations such as distillation,[8] adsorption,[9] extraction,[10] and crystallization.[11] Membranes can be utilized not only to replace existing unit operations but to improve and synergistically supplement them. The compact design and easy operation of membrane

Correspondence concerning this article should be addressed to Y.M. Lee at ymlee@hanyang.ac.kr and E. Drioli at e.drioli@itm.cnr.it.

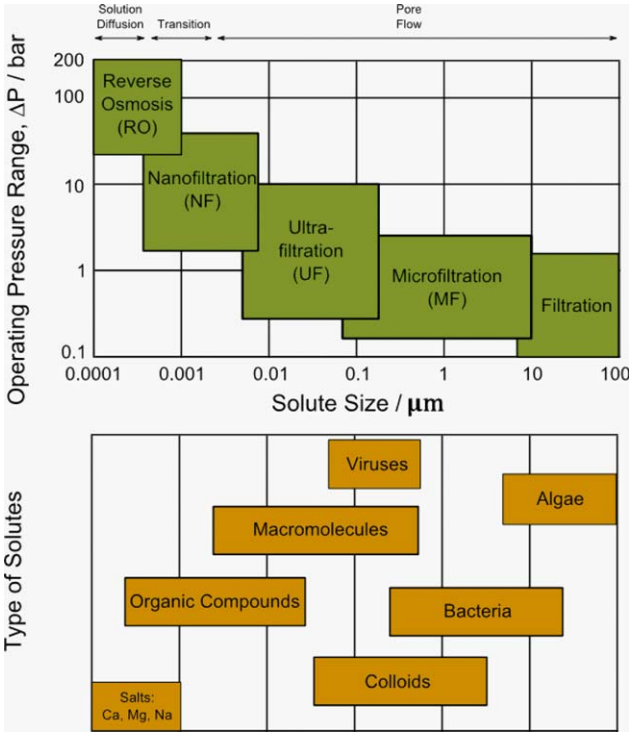

Figure 1. Different types of membrane processes.

[Color figure can be viewed in the online issue, which is available at wileyonlinelibrary.com.]

processes meet the basic principles of process intensification strategies.[12]

The market prospects for membrane technology are also promising. The current market size is approximately $20 billion, with a fast growth rate of 8% expected to 2018.[13] With water and energy shortages being two of the main challenges of the future, it is likely that membrane processing will continue to be an important technology.

To meet the growing market demands, decades of membrane research have produced many interesting new materials and diverse methods to fabricate high performance membranes along with advanced module fabrication technology and optimized process operation. There exists an in-depth understanding of membrane formation mechanism from the thermodynamic and kinetic perspectives, and it is now possible to fine-tune the final membrane morphologies including the pore size, pore interconnectivity, presence of macrovoids, and porosity, to maximize the membrane performance. Apart from the membrane formation techniques, module fabrication and process operation are two key aspects for successful commercialization of membrane technology. Two of the commonly used membrane modules are spiral wound modules and hollow fiber modules. There have also been many breakthroughs in terms of process operation such as the adaptation of pressure exchangers to reduce energy consumption,[1] constant-flux operation mode to minimize fouling,[14] and innovative process schemes to maximize process productivity.[15,16]

With the advent of better membrane fabrication methodologies, (i.e., advanced materials with improved control of membrane morphologies), the applications of membrane technology are continuously becoming wider. For instance, the emergence of organic solvent nanofiltration[17,18] and perva-poration[19,20] technology now allows for nonaqueous membrane systems for use in pharmaceutical, fine chemical, and petrochemical industries where organic media are commonly used to handle their products. As separation of chemical processes accounts up to 70% of the total production cost,[21] the impact that membrane technology can bring to such industries is likely to be significant.

Another very interesting and emerging application field is the membrane contactor technology.[22] The membrane in this application does not act as a selective barrier but as a layer that separates two phases, and the membrane facilitates the transport of solutes from one side to another in a controlled manner. Several commercial scale membrane contactor units exist now in operation in aromatic recovery and selective removal of heavy metals from a galvanic process bath.[23,24] Some of the developing applications include membrane distillation (MD), membrane crystallization (MCr), membrane condensers, and membrane emulsifiers. The interesting feature about the membrane contactor technology is that hydrophobic microporous membranes are used, which is rather unconventional because hydrophilic membranes are generally preferred in conventional applications due to their higher flux and low fouling tendency.

As illustrated in Figure 2, MD utilizes a hydrophobic membrane that prevents transfer of liquids while allowing the vapor phase to permeate due to a vapor pressure gradient. As no osmotic gradient can act between the two opposite phases, MD offers an alternative method to further desalinate brine solutions without pressurizing the liquid, and has 100% theoretical rejection of nonvolatile compounds. As the membrane should not be wetted during continuous operation, high hydrophobicity and narrow pore size distribution are critical surface parameters that must be controlled to achieve stable long term performance. Hence, the basic requirements for suitable MD membranes are high porosity with narrow pore size distribution, low thermal conductivity, and good mechanical and thermal stabilities.

The concept of MCr is similar to that of MD. That is, a microporous hydrophobic membrane is used to concentrate a solution via vapor pressure gradient in a controlled manner. Crystallization is a common unit operation and is well established in the chemical industries. However, with the market trend shifting from base chemicals toward life-science products, there are still high demands for better crystallization processes with finer control and higher product quality.[22] A unique feature of MCr is that the membrane provides

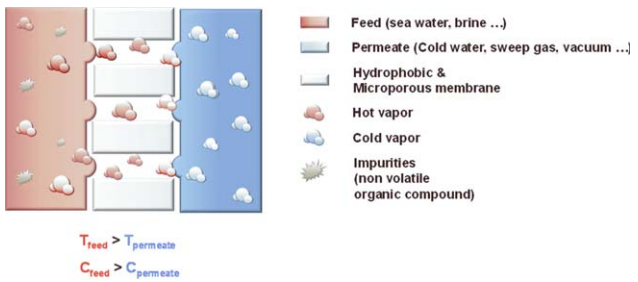

Figure 2. Basic schematic of membrane distillation process: hydrophobic microporous membrane acts as a barrier and allows vapor to permeate via vapor pressure gradient.

[Color figure can be viewed in the online issue, which is available at wileyonlinelibrary.com.]

Table 1. Main Fluoropolymers Used to Prepare Membranes[29]

Polymer	Chemical Structure
PVDF	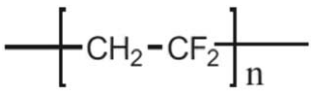
PVDF-*co*-HFP	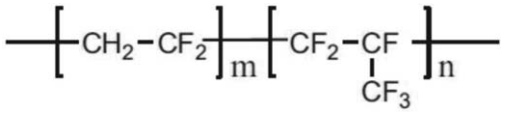
PVDF-*co*-TFE	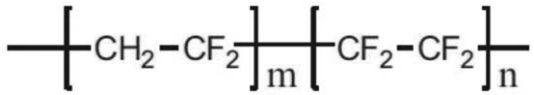
PVDF-co-TrFE	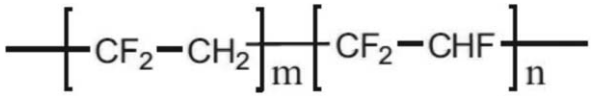
PTFE	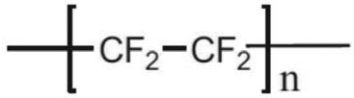
ECTFE (Halar®)	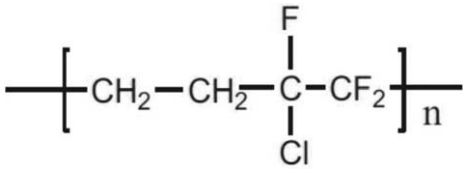
Hyflon® AD	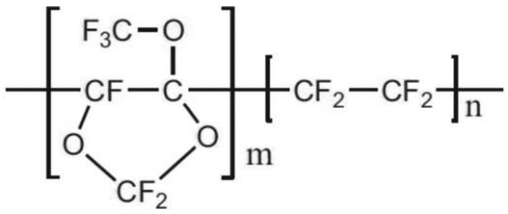

heterogeneous nucleation sites which allow delicate control of the crystal purity, size, nucleation kinetics, and importantly, polymorphism.[25] For instance, previous works have shown that the polymorphic structures of crystalline materials can be tailored using membranes by controlling the supersaturation state.[26]

For most of the emerging membrane contactor applications, the key hurdle that limits their commercialization is the membrane itself. As most membrane developments until now have been focused on other applications, there is an urgent need to develop suitable membranes that can push such processes to the industrial level. To keep pace with new developing applications, more advanced materials and methodologies need to be developed.

Currently, the main fabrication platform is the nonsolvent induced phase separation (NIPS) method which is versatile, convenient, and scalable.[27] However, with the advent of new emerging applications, different methods such as the thermally induced phase separation (TIPS) and electrospinning methods are gaining momentum due to their unique ability to fabricate tailored membranes. More recently, a new method combining the advantages of NIPS and TIPS (N-TIPS) has been reported by several researchers. This emerging method deserves special attention as it may allow fabrication of highly porous skin layers with mechanically robust supports.[28,29] In this review, we assess the current understanding of membrane fabrication knowledge with a particular focus on controlling the membrane morphology and surface chemistry using the TIPS and electrospinning methods for potential application in membrane contactor applications.

Membrane Materials

In the past several decades, several membrane materials have been researched including: polymeric, ceramic, metal, and carbon membranes.[14] Among the materials, polymeric membranes currently dominate most of the markets due to

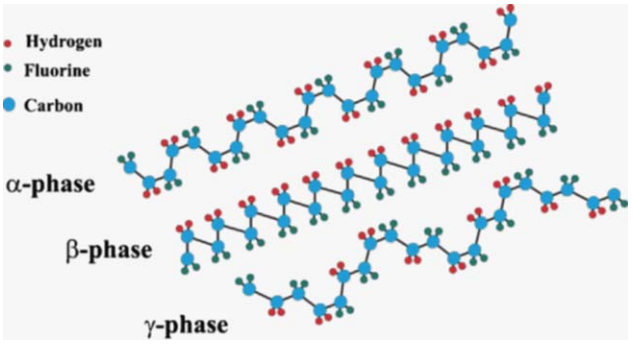

Figure 3. Representation of PVDF conformation and α, β, and γ phases.[37]

[Color figure can be viewed in the online issue, which is available at wileyonlinelibrary.com.]

Table 2. List of PVDF Membranes Prepared with the TIPS Method

Year [Ref.]	Solvent	Additive	Flat/HF	Structure	Polymorphism	Tensile (MPa)	Elongation (%)	PWP ($L.M^{-2}.hr^{-1}.bar^{-1}$)	Porosity (%)	Pore Diameter (μm), Solute Rejection (%)
2006 Li et al.[81]	DBP	$CaCO_3$	Flat	Cellular (with $CaCO_3$) Spherulitic	–	4–15	–	–	10–50	–
2006 Gu et al.[82]	DMP, DBP, DOA, DOS	–	Flat	Spherulitic	–	–	–	–	42–68	–
2006 Cha et al.[83]	GBL	PVP	HF	Spherulitic	γ-phase (with PVP)	–	250–350	600–1100	–	R > 90% (100 nm PS particle)
2006 Gu et al.[84]	DMP	–	Flat	Spherulitic	α-phase	–	–	–	–	–
2007 Ji et al.[85]	DBP/DEHP	–	Flat	Spherulitic	–	–	–	–	–	—
2007 Su et al.[86]	GBL/CO, CO/DBP	–	Flat	Spherulitic sheaf-like	α-phase, γ-phase	0.2–2	–	400	70	–
2008 Cui et al.[87]	Sulfolane	PMMA	Flat	Cellular (with PMMA), Spherulitic	–	–	–	–	–	–
2008 Rajabzadeh et al.[88]	Triacetin	Glycerol	HF	Spherulitic	–	1–4	–	50–700	–	R = 68–95% (20 nm polystyrene particle)
2008 Gu et al.[89]	Benzophenone	–	Flat	Spherulitic	α-phase	–	–	–	–	–
2008 Yang et al.[90]	DPK	–	Flat	Cellular Spherulitic	–	0.32–1.60	–	–	–	0.09–0.54
2008 Li et al.[91]	DBP/DOP	–	Flat	Spherulitic Cellular	α-phase, γ-phase	–	–	–	–	–
2009 Rajabzadeh et al.[92]	Triacetin	PMMA	HF	Spherulitic	β-phase, α-phase	–	40–120	50–200	70–74	–
2009 Lu et al.[93]	DBP/DOP	–	Flat	Spherulitic	–	–	–	50–350	65–80	–
2009 Lin et al.[94]	DPC/DMAc	–	Flat	Cellular Spherulitic	–	2–14	–	–	20–80	–
2010 Cui et al.[95]	DBP	SiO_2	Flat	Spherulitic	–	7–14	100–350	40–140	45–65	–
2010 Yang et al.[96]	PGC, DPK, DMP, DBP	–	Flat	Spherulitic Cellular	α-phase (DPK, DMP, DBP), β-phase (PGC),	–	–	–	–	–
2011 Ghasem et al.[97]	Triacetin	Glycerol	HF	Spherulitic	–	15–27	20–40	0–70	70	4–13
2012 Rajabzadeh et al.[98]	DEP	PVP PMMA	HF	Spherulitic	–	2–7	100–700	50–2000	–	R = 40% BSA
2013 Li et al.[99]	DOP	–	HF	Cellular	–	3–5	110–200	270–280	66–70	–
2013 Liang et al.[100]	$DMSO_2$	–	Flat	Tubular needle-like pores	–	–	–	–	–	–
2013 Zhang et al.[101]	TEP	–	HF	Spherulitic	α-phase, β-phase	–	–	–	–	–
2013 Cui et al.[102]	ATBC	–	Flat/HF	Spherulitic	α-phase	0.9–4.8	10–15	500–4500	65–76	0.27–0.56
2014 Hassankiadeh et al.[103]	ATBC	–	HF	Spherulitic	α-phase	2–5	50–80	100–2000	60–75	0.18–0.22
2014 Wu et al.[104]	DPC/DMAc	PES-C	Flat	Spherulitic Cellular	–	–	–	120–210	68–72	–
2014 Wang et al.[105]	GBL/DOP	–	HF	Cellular, Sponge-like	–	3–7	–	300–2000	60–80	0.2–0.4
2015 Cui et al.[106]	TEGDA	–	flat	Fibrillar	α-phase	0.6–2.1	20–470	600–2300	68–75	0.11
2015 Hassankiadeh et al.[29]	Polarclean	PVP PMMA Glycerol	HF	Spherulitic	α-phase, β-phase	1–6	20–40	100–1000	60–70	–
2015 Xu et al.[107]	NMP	PFSA	Flat	Asymmetric	β-phase	–	–	200–500	83–90	–
2015 Wang et al.[108]	TEP/DCAC	–	Flat/HF	Spherulitic Cellular	α-phase	0.5–3	–	100–2000	56–70	0.01–0.43
2015 Sawada et al.[109]	ATBC, ATEC, TEC	–	Flat	Fibrillar Spherulitic	α-phase	0.3–0.6	30–60	8200–11,000	52–76	0.9–7.2
2015 Lee et al.[28]	GBL, DMAc	LiCl Glycerol PVP	HF	Spherulitic	–	4–6	–	500–1600	61–64	–

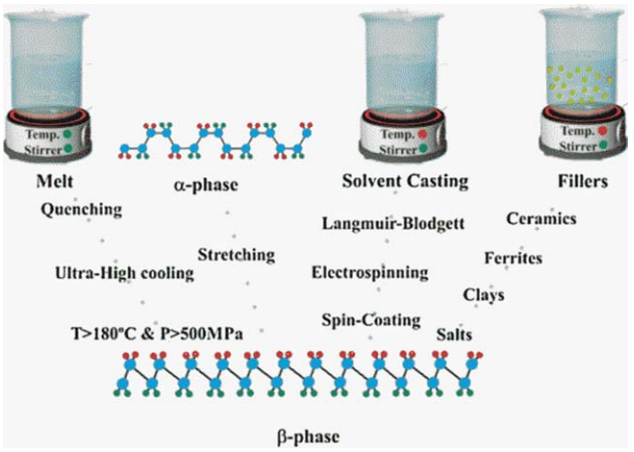

Figure 4. Different strategies to obtain beta-phase PVDF.[37]

[Color figure can be viewed in the online issue, which is available at wileyonlinelibrary.com.]

their low cost and easiness of module fabrication. Extensive reviews for membrane polymeric materials can be found in the literature.[30–32] Among the polymeric membranes, fluoropolymers have been widely used since the 1980s due to their excellent mechanical strength, chemical and thermal stabilities, and chemical diversity, as summarized in Table 1. Although the main focus of membrane research has been on hydrophilization of fluoropolymers for use in water applications,[33] fluoropolymers are intrinsically hydrophobic, making them excellent candidates for membrane contactor applications.

Polyvinylidene fluoride (PVDF) is one of the most widely used fluoropolymers for membrane applications. Initially, PVDF was used due to its chemical inertness and good solubility in aprotic solvents (DMF, NMP, DMAc), which makes it an excellent material for membrane preparation. More recently, many unique intrinsic features of PVDF are being exploited for membrane applications. PVDF is a semicrystalline polymer with a typical crystallinity between 35 and 70%.[34] The glass transition and melting temperatures of the polymer are in the ranges of −40 to −30°C and 155 to 192°C, respectively. The crystalline phase of PVDF has three different molecular conformations and the polymer can exhibit a combination of five distinct crystal polymorphs: α, β, γ, δ, and ε-phases depending on its thermal mechanical history.[35,36] Among the possible polymorphs, α, β, and γ-phases are the most common phases, as shown in Figure 3.

Previous works have shown that the polymer intrinsic properties such as dielectric constant, ferroelectric properties, and polarity are significantly affected by the polymorphism.[37] Also, among the three common phases, the β- and γ-phases exhibit interesting electroactive properties with the β-phase showing the highest dipolar moment per unit cell (8×10^{-30} C m).[38] In most PVDF membranes, the α-phase form is the most frequently observed phase as it is a kinetically favorable phase,[39] whereas the β-phase is thermodynamically more stable and is seldom observed in membranes.

Although not fully elucidated yet, such drastic differences in polymorphism may have a significant effect on the final membrane performance in terms of membrane fouling and membrane wetting. For instance, Coster et al.[40–42] fabricated PVDF membranes with piezoelectric properties by inducing a β-phase polymorph and reported enhanced antifouling properties in these membranes. Unfortunately, the polymorphism effect has largely been neglected in the membrane literature and many of the studies on PVDF membranes lack detailed characterization of the PVDF phases (Table 2). Nevertheless, polymorphism is now being highlighted as an important factor, and recent publications have started to include the polymorphism data of the fabricated membranes (Table 2).

In the field of polymer chemistry, different methods have been developed to control and tailor the PVDF polymorphism to the β-phase via specific procedures and the inclusion of specific fillers and nucleating agents, as illustrated in Figure 4. With respect to the membrane fabrication, Yu et al.[43] induced β-phase in PVDF/CNT composite membranes using a sonication method. Gregorio et al.[44] found that crystallizing PVDF from DMF or DMAc at temperatures below 70°C results in the formation of the β-phase. Also, techniques like corona charging or electrical poling also converted PVDF from α- to β-phase.[45–47] Stretching PVDF membranes at 50–145°C has also shown to be a simple and effective technique to realign the polymer to β-phase.[48] However, it is still difficult to fine-tune the polymer polymorphism because the crystallization kinetics are sensitive to different parameters.

Apart from the PVDF homopolymer, different PVDF copolymers have also been developed with different properties. A recent review summarizes different PVDF copolymers for membrane applications.[31] Among the possible copolymers, PVDF-HFP, first reported in 2007, is particularly promising because the fluorine groups in the HFP increases the overall hydrophobicity of the material while maintaining its solvent solubility.[49,50] Other PVDF copolymers for membrane applications include PVDF-*co*-TFE[51] and PVDF-*co*-TrFE.[52,53]

PTFE, well known under the trademark Teflon®, exhibits remarkable chemical stability, mechanical strength, and thermal resistance. PTFE also has a lower surface energy and a higher hydrophobicity compared to other fluoropolymers, making it an ideal candidate for membrane contactor applications. However, as no known solvent dissolves PTFE at room temperature, it is very difficult to process into a membrane. PTFE membranes are typically fabricated using melt processing techniques but its high melt viscosity has made it difficult to produce reliable membranes.[54] Conventional techniques include extrusion of polymer blends followed by sintering to obtain PTFE membranes, yet the performance is unexpectedly lower than that of membranes prepared using other conventional materials.[55–57] Nevertheless, there has been interesting breakthroughs in PTFE membrane fabrication techniques[58] where a PTFE emulsion was made into a handleable paste at high shear rate with subsequent extrusion at low temperatures (~90°C) without any additives.

Polyethylene chlorotrifluoroethylene (ECTFE) (trademark Halar®) is a new emerging type of polymer with interesting properties and is relatively unexplored as a membrane material. The melting point of ECTFE is between 200 and 260°C, and it has excellent chemical and thermal stability, allowing continuous operation at temperatures higher than 150°C in harsh chemical conditions.[31] ECTFE is also very hydrophobic and has potential for membrane contactor applications. In addition, like PTFE, ECTFE does not dissolve in any known solvent at ambient temperatures; however, ECTFE becomes soluble in certain solvents at elevated temperatures, allowing it to be fabricated into membranes via the TIPS method. Hence, selecting the right solvent is the key factor in ECTFE membrane research. There are relatively few research papers

Table 3. List of ECTFE Membranes Prepared with the TIPS Method

Year	Solvent	Additive	Flat/HF	Structure	Tensile (MPa)	Elongation (%)	PWP ($L.M^{-2}\ h^{-1}\ bar^{-1}$)	Porosity (%)	Pore Diameter (μm)
2002 Ramaswamy et al.[59]	TCB, DBP, DOP		Flat	Spherulitic			Ethanol, 10–20		0.4–0.6
2010 Roh et al.[60]	DBP		Flat	Spherulitic			IPA, 2–15		0.07–0.34
2012 Simone et al.[62]	NMP	GTA, Citroflex, DEA, DBI	Flat	Spherulitic, dense	14–18	5–30	27–157		
2014 Drioli et al.[110]	GTA		Flat	Spherulitic, dense				80–85	0.02–0.1
2015 Pan et al.[111]	DOA	SiO_2, Composite powder	Flat	Cellular	4.5–5.5	35–45	83–255	57–76	0.07–0.42

on ECTFE membranes[59–62] (Table 3) but with the advent of membrane contactor applications, this is likely to increase in the future.

Hyflon® AD is a hydrophobic *amorphous* glassy fluoropolymer with exceptionally high fractional free volume and high gas permeability. It has excellent chemical stability and high solubility in perfluorinated solvents (i.e., Galden® HT 55), rendering the polymer suitable for membrane fabrication. In addition, its hydrophobicity and high free volume make it promising for membrane applications. It has been coated onto PVDF membranes with narrow pore size distribution and high overall porosity.[63–65] Like ECTFE, not much work has been done on this unique polymer, and future research activity is likely to be focused on membrane contactor applications.

Membrane Fabrication Methods

Polymeric membranes can be fabricated using several different methods including phase inversion, melt extrusion, controlled stretching, electro-spinning, and track etching.[14,66] Currently, the phase inversion method is the most common type due to its versatility and scalability. The phase inversion method is also referred to as the phase separation or polymer precipitation method. Phase inversion is a demixing process where a polymer dope solution is first phase separated into a polymer rich and polymer lean phase with subsequent solvent removal to form a solid membrane. To control the final membrane morphology, one needs to have an in-depth understanding of solution thermodynamics and demixing kinetics. Abundant literature is available on the theoretical foundations of phase inversion including descriptions of phase diagrams and demixing paths; however, in practice, this process is largely empirical with a heuristic approach being adopted.

There are four main types of phase inversion methods: TIPS, NIPS, vapor induced phase separation (VIPS), and solvent evaporation. Among the phase inversion methods, TIPS and NIPS are the most widely used methods. As the NIPS method has been extensively reviewed recently,[27,67] it will not be covered in detail in this review. Apart from the phase inversion methods, the electrospinning method has been gaining considerable interests from researchers for membrane contactor applications. The electrospinning technique is being widely applied to many different polymers due to its ability to prepare highly porous membranes with narrow pore size distributions and low tortuosity.

In this review, the TIPS and electrospinning methods are discussed, as these two methods have the potential to meet the needs of the emerging membrane applications in terms of morphology and surface chemistry control. In addition, the NIPS method is also briefly covered to discuss the combination of the NIPS and TIPS method (N-TIPS method).

Thermally Induced Phase Separation

TIPS was first introduced and researched in the 1980–90s[68–76] to fabricate microporous membranes, but it has not gained much attention as NIPS was deemed as a more convenient and versatile method to prepare polymeric membranes. Recently, however, with the advent of membrane contactors, TIPS research is regaining its momentum due to many unique advantages such as process simplicity, high reproducibility, low tendency to form defects, high porosity, and the ability to form interesting microstructures with narrow pore size distribution. In addition, the ability to control the polymer

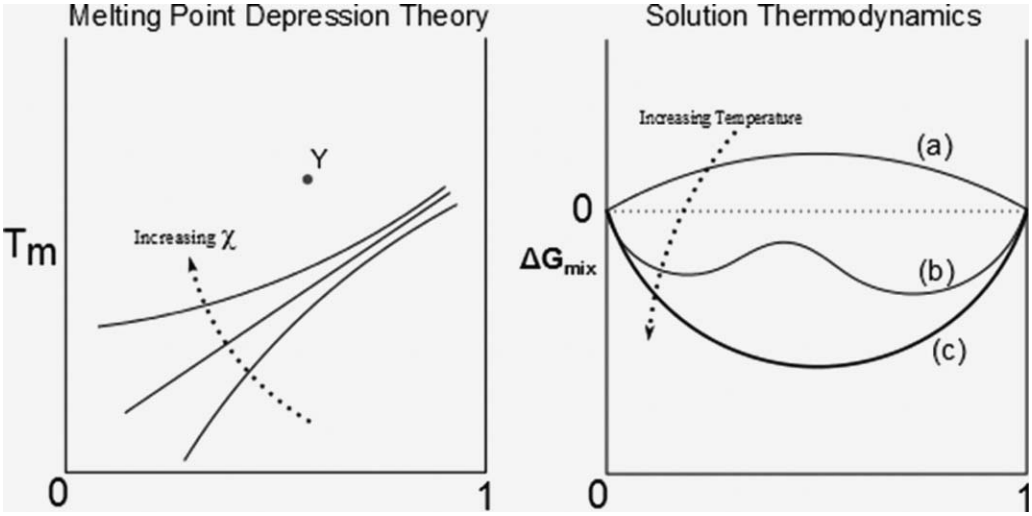

Figure 5. (Left) Temperature-composition phase diagram for a hypothetical semicrystalline polymer at three different χ values.[70] Three lines represent the melting point depression curve and point *Y* represents a stable homogeneous state. (Right) Gibbs free energy of mixing against polymer volume fraction: (a) immiscible ($\Delta G_{mix} > 0$), (b) partially miscible, (c) miscible.[71]

polymorphism using solvents and process parameters is being highlighted as a unique feature.

The basic procedure for the TIPS method is as follows[70]:

1. Dissolve a polymer of interest in a high-boiling, low MW solvent at an elevated temperature, typically near or higher than the melting point of the polymer to form a homogeneous melt-blend.
2. Cast the dope solution into the desired shape, for example, flat-sheet or hollow fiber.
3. Cool the cast solution in a controlled manner to induce phase separation and precipitation of the polymer.
4. Extract the diluent, often via solvent extraction, to yield a membrane.

As described, the membrane is formed from a homogeneous dope solution by removing the thermal energy to induce phase separation. Hence, the phase inversion process is a delicate balance between the polymer–solvent interaction, cooling rate, cooling media, and thermal gradient. As pointed out by Lloyd et al.,[70] one of the distinct advantages of the TIPS method is the ability to fabricate membranes from semicrystalline polymers that are not usually soluble in solvents at ambient temperatures (e.g., ECTFE). In addition, the TIPS process is usually a binary system, as compared to the ternary NIPS system, rendering the TIPS process inherently simpler than the NIPS with fewer variables to be controlled. Conversely, the TIPS method is relatively more energy intensive compared to the other phase inversion methods. And the simplicity of the TIPS method could limit the possible application range of the fabricated membranes (e.g., not applicable to reverse osmosis); however, it will be shown in later sections that the combination of NIPS and TIPS (N-TIPS) could offer viable solutions to overcome such limitations by offering greater degrees of freedom in fabrication parameters.

Theoretical development

All of the phase inversion processes (NIPS, TIPS, and VIPS) can be described using the same thermodynamic principles: a thermodynamically stable dope solution is exposed to an unstable environment where it is *demixed* and ultimately precipitates into a solid membrane. Hence, the compatibility between the polymer and the solvent, or the thermodynamic stability, is a critical factor for the phase inversion processes.

As most TIPS polymers are semicrystalline (e.g., polypropylene, polyethylene, and PVDF), the starting point for theoretical consideration is melting point depression theory together with the Gibbs free energy of mixing. Depending on the compatibility between the polymer and the solvent, the melting point can decrease, or depress, which can be related to the phase stability via thermodynamic relationships. The melting point depression equation can be described using the Flory–Huggins theory as follows

$$T_m = \frac{1}{\frac{RV_u\left(\varnothing_d - \chi\varnothing_d^2\right)}{\Delta H_u V_d} + \frac{1}{T_m^\circ}} \quad (1)$$

where T_m and T_m° are the melting temperatures of the polymer in the dope solution and the pure crystalline polymer, respectively, and V_d and V_u are the molar volumes of the solvent and the polymer repeat unit, respectively. ΔH_u represents the heat of fusion for the repeat unit, $\varnothing_d$ is the volume fraction of the solvent, and χ represents the Flory–Huggins interaction parameter.

As the value of χ increases, the strength of the polymer–solvent interaction decreases, and vice versa. Equation 1 reveals several important traits. First, Eq. 1 indicates that melting point depression increases with smaller solvent molar volumes and smaller ΔH_u values. This is an important inference as it narrows the choice of the potential solvents. Also, when Eq. 1 is plotted against polymer volume fraction ($\varnothing_P = 1 - \varnothing_d$) with different χ values (different diluents), the thermodynamic stability of a dope solution can be clearly represented, as shown in Figure 5.

The calculated lines at three different χ values roughly represent the transition temperature at which the dope solution begins to phase separate (note T_m is higher than T_c). If the χ value is small, then the dope mixture undergoes solid-liquid phase separation via polymer crystallization. Conversely, when the χ value becomes larger a convex curvature is observed (Figure 5). In such a polymer-solvent system, the phase separation can proceed via liquid-liquid demixing

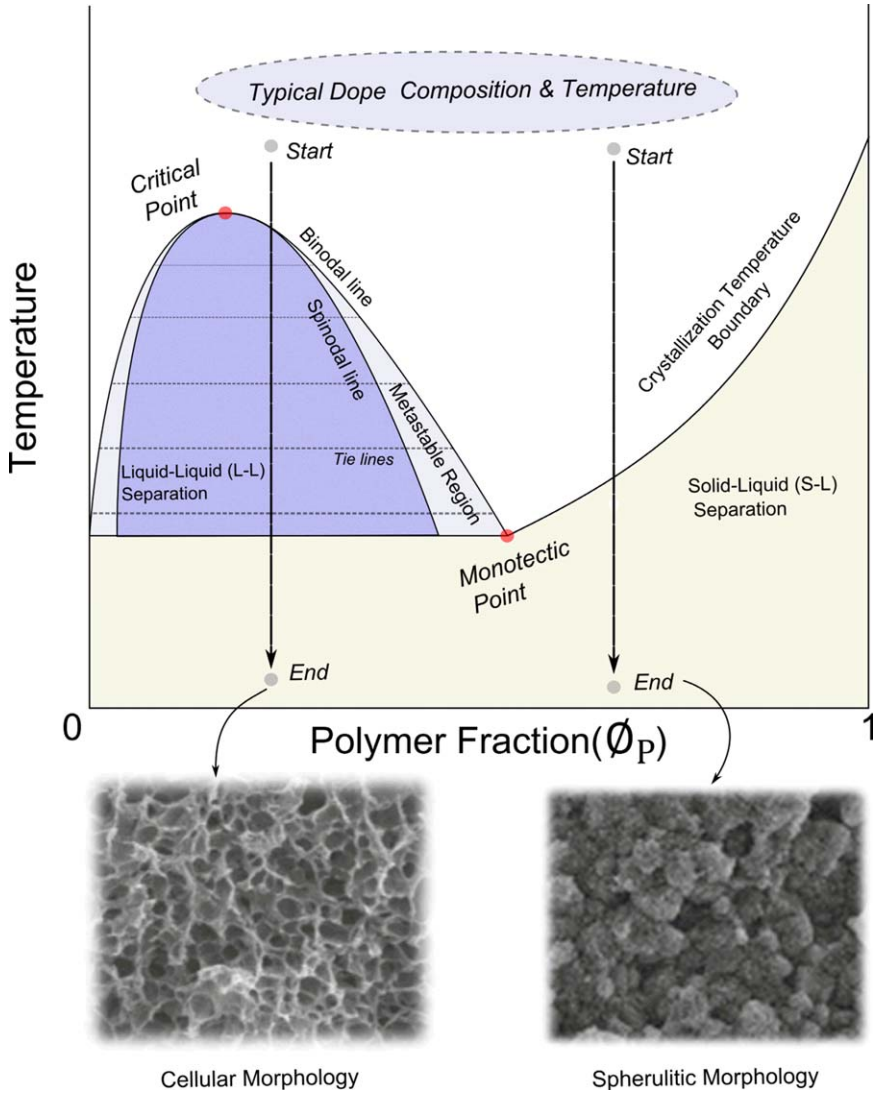

Figure 6. Characteristic phase diagram of TIPS process.

[Color figure can be viewed in the online issue, which is available at wileyonlinelibrary.com.]

followed by polymer solidification, yielding highly porous microporous membranes. As will be discussed later, controlling the liquid-liquid demixing kinetics is critical to fine-tuning the final membrane morphology.

Melting point depression theory can be combined with solution equilibrium thermodynamics[71] to better describe the phase stability of dope solutions. Early researchers on TIPS have adopted a two-dimensional phase diagram to better represent the TIPS process,[77] as illustrated in Figure 6 ($\chi \gg 0$).

Once a stable dope solution (marked as *start* in Figure 6) at high temperature is cooled at a controlled rate, it follows the path shown in arrows. At high polymer fractions, typically above 30%, the membrane passes through the crystallization temperature boundary, and the phase separation proceeds via solid-liquid (S-L) separation where the polymer crystallizes directly from the dope solution. Conversely, at relatively lower polymer fractions, the dope solution first enters the metastable region where liquid-liquid (L-L) demixing takes place. Inside the L-L separation region, the dope solution phase separates into a polymer-poor phase and a polymer-rich phase along the tieline. The polymer-rich phase forms a continuous polymer phase, which eventually becomes the membrane, and the polymer-poor phase becomes the pores of the final membrane.

To understand the phase inversion process theoretically, several researchers have applied simulation methods. Hanks et al.[78] reported a deterministic simulation model of liquid-liquid separation revealing the polymer matrix formation process (Figure 7). Another work by Mino et al.[79] used phase field separation model gives insight into the phase demixing mechanism. As the phase separation phenomena is in-between atomic and macroscopic scale, He et al.[80] applied a dissipative particle dynamics simulation to perform mesoscopic analysis of phase separation mechanism.

The membranes formed by these two pathways show distinctly different morphologies as shown in Figure 6. Typically, membranes formed through the L-L separation pathway exhibit a porous honeycomb-like cellular morphology (also referred to as bicontinuous morphology), whereas membranes formed via the S-L separation pathway show fuzzy spherulitic (sphere-like) structures. Apart from the macroscopic morphology, that is, cellular and spherulitic, the size of the spherulites is highly dependent on the fabrication conditions including cooling rate, temperature gradient, and inclusion of additives. It is worth noting that different morphologies result in drastically different properties in terms of flux and mechanical properties.

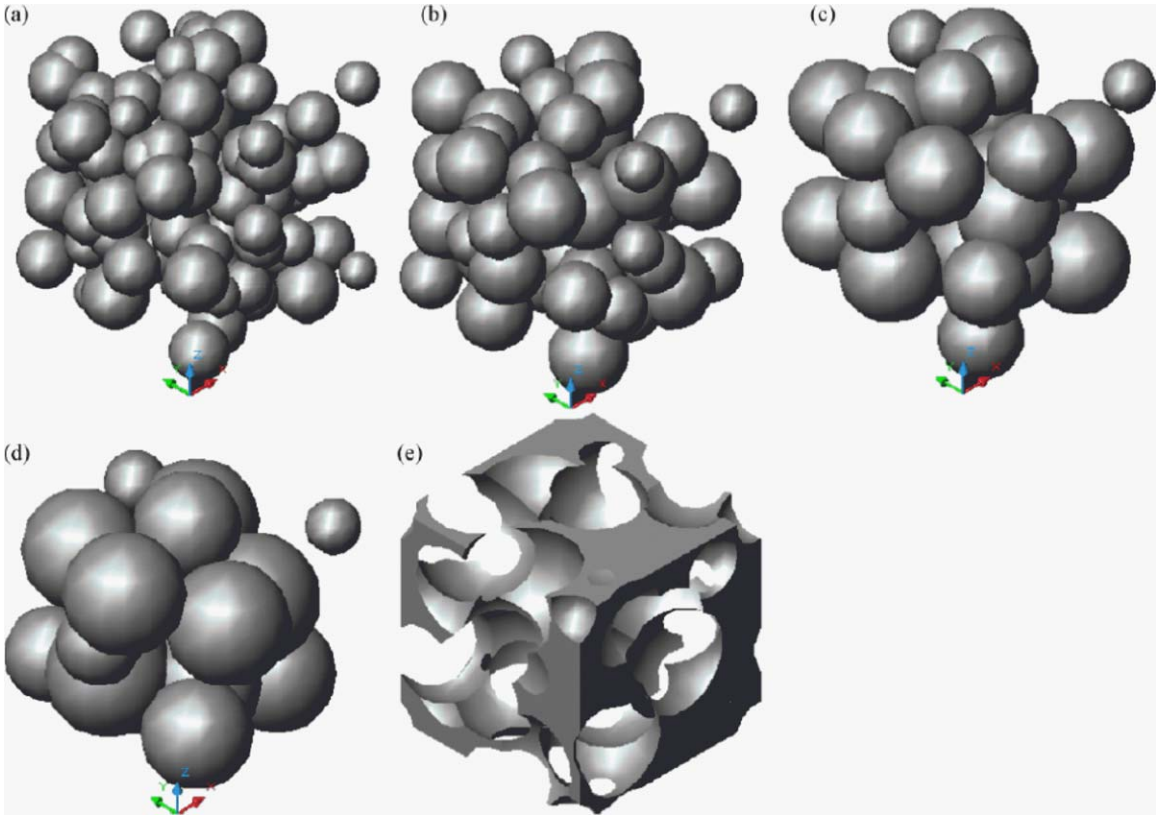

Figure 7. Simulation of polymer solidification process during liquid-liquid phase separation. (a–d) Show the simulated growth of the polymer-lean droplets (which eventually become membrane pores) with time, and (e) shows the final polymer matrix phase at the end of the simulation.[78]

[Color figure can be viewed in the online issue, which is available at wileyonlinelibrary.com.]

The monotectic point shown in Figure 6 is the point at which the binodal line meets the crystallization temperature boundary. L-L separation is induced below this monotectic point, and S-L separation occurs above the monotectic point. The point where the spinodal line and the binodal line meet is called the critical point. Identifying the critical point is important in membrane fabrication because, if the initial polymer content in the dope solution is lower than the critical point, the phase separation results in a continuous solvent-rich phase and a discontinuous polymer-rich phase, ultimately forming powders instead of a membrane. Hence, it is important to prepare dope solutions with concentrations above the critical point. Apart from the dope composition and the temperature, parameters such as cooling rate, solvent–polymer interaction, and choice of nucleating agent can significantly affect the membrane morphology. Understanding and controlling such effects is critical for tailoring the membrane performance for membrane contactor applications.

Tables 2 and 3 summarize the reported literature on fabricating TIPS membranes using fluoropolymers with different solvents, temperature profiles, and additives. Understanding and relating the process parameters to the final membrane morphology can be difficult and requires careful interpretation. The resulting membranes show drastically different properties in terms of pore size, flux, and mechanical strength. Additionally, the crystal polymorphism is affected by the fabrication method.

There are many studies related to the effect of polymer–solvent interactions on the final membrane morphology; unfortunately, the majority of the reported literature provide the structure and mechanical analyses without reporting the actual membrane performance (flux and rejection), and they do not suggest a clear direction for further improvements. In this review, we attempted to compile the literature data for fluoropolymer membranes prepared via TIPS to assess the current status of TIPS-prepared membranes.

Effect of polymer–solvent interaction

Selecting the right solvent, or diluent, is one of the key criteria for the TIPS process. The words "solvent" and "diluent" are used interchangeably in this review and in the TIPS literature. As one can expect, it is rather difficult to choose an appropriate TIPS solvent. A suitable solvent should have a high boiling temperature, low molecular weight, low toxicity, low environmental impact, low cost, and reasonable compatibility with the polymer over a wide temperature and concentration range. In addition, as mentioned previously, the thermal conductivity as well as the miscibility with the quenching media are also important factors influencing the final membrane morphology.

The compatibility between the solvent and the polymer shapes the phase diagram of the system, as it determines the location of the binodal curve and polymer crystallization temperature of the mixture. For instance, the binodal curve shifts to higher temperature with decreasing compatibility, and vice versa. The solvent–polymer compatibility can be semiquantitatively approximated using the solubility parameter.[112]

In TIPS process, solvents with similar chemical functionalities can yield drastically different results. For instance, Yang et al.[90] proposed diphenyl ketone (DPK) solvent to prepare

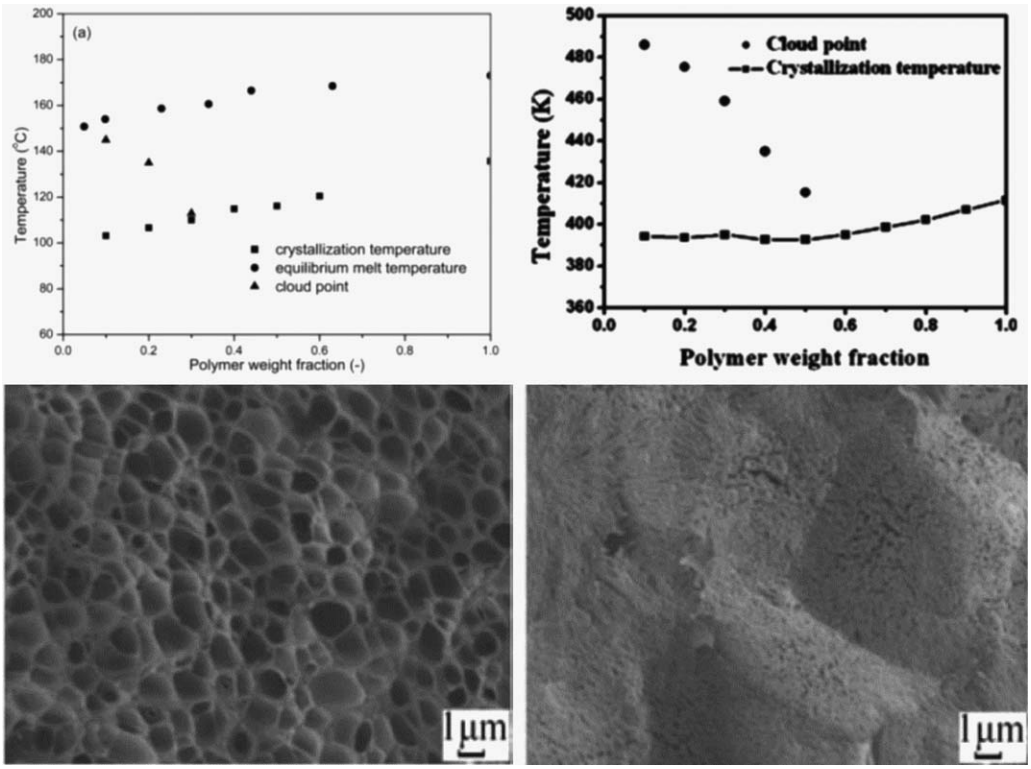

Figure 8. (Top left) Phase diagram of PVDF/DPK system,[90] monotectic point is at about 30 wt %. (Top right) Phase diagram of PVDF/DPC system,[94] monotectic point is at about 50 *wt*%. (Bottom left) Cross sectional structure of PVDF-DPC membranes prepared by quenching into ice water: 40 wt % PVDF showing bicontinuous morphology. (Bottom right) 50 wt % PVDF showing spherulitic morphology.[94]

PVDF membranes by TIPS method. The monotectic point of the mixture was approximately 30 wt % (Figure 8). From the same group, Lin et al.[94] used diphenyl carbonate (DPC) as a new solvent to prepare PVDF membranes by the TIPS method. Surprisingly, the monotectic point of the mixture was determined to be 56 wt %, allowing liquid-liquid separation with high polymer concentration. Considering that the chemical structure of DPK and DPC are not very different, such a drastic difference in the phase diagram highlights the importance of polymer–solvent interactions. The drastic change from L-L separation to S-L separation is clearly visible in the reported SEM data. As expected, porosity decreased and mechanical strength increased with increasing polymer concentration. Polymorphism data were not reported.

Hassankiadeh et al.[103] investigated the effect of polymer molecular weight on the final membrane performance for a PVDF/tributyl O-acetyl citrate (ATBC) binary system. Hollow fiber membranes were fabricated using the TIPS process with different PVDF molecular weights and different preparation conditions. It was observed that the binodal line slightly shifted down with decreasing polymer molecular weight. Conversely, lower molecular weight PVDF reduced the dope solution viscosity, which increased the overall membrane porosity but decreased the mechanical strength. Interestingly, a very

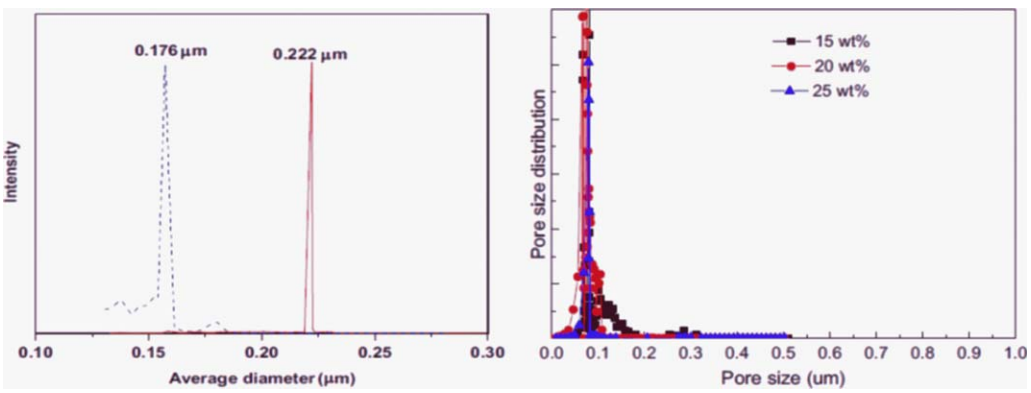

Figure 9. (Left) Mean pore size distribution of HF membranes prepared using PVDF/ATBC system via TIPS.[103] (Right) PVDF/TEGDA system via TIPS.[106]

Very narrow pore size distributions are obtained using TIPS method. [Color figure can be viewed in the online issue, which is available at wileyonlinelibrary.com.]

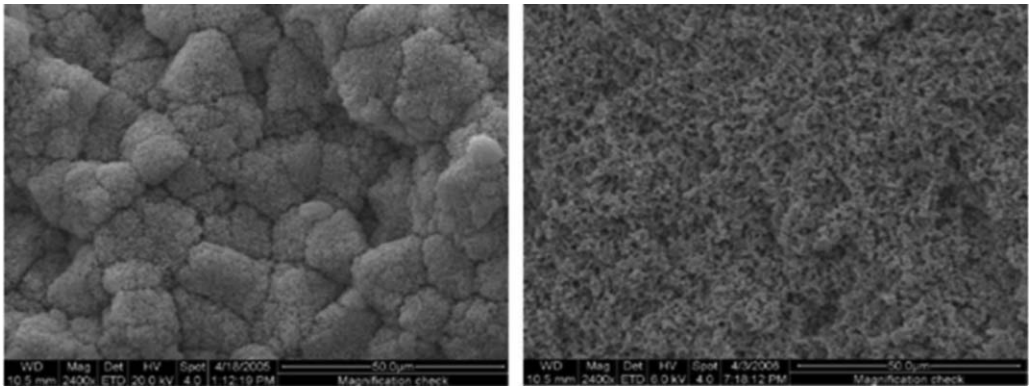

Figure 10. Effect of DBP/DOP ratio in 30 wt % PVDF membrane structure. (Left) 9/1 ratio resulted in spherulitic structure, (right) 4/6 resulted in cellular structure.[91]

sharp pore size distribution was obtained (Figure 9), and the distribution was independent of the polymer molecular weight. The polymorphism of the prepared membranes was primarily α-phase regardless of the preparation conditions, indicating that the polymer–solvent interaction is the key factor that determines the PVDF phase in the TIPS process. More citrate-based solvents have been reported recently.[109]

As the TIPS method is generally used in a binary system, the degrees of freedom for structural control are rather limited. Hence, to obtain better control of the membrane structure and performance, many authors used solvent mixtures to prepare PVDF membranes by TIPS. Solvent mixtures such as dibutyl phthalate (DBP)/di-(2-ethylhexyl phthalate (DEHP),[85] DBP/dioctyl phthalate (DOP),[91] dimethyl phthalate (DMP)/dioctyl adipate (DOA),[82] DMP/DOP,[82] DOP/γ-butyrolactone (GBL),[105] and triacetin/glycerol[88] have been reported. The works have shown that the position of the binodal line can be changed by introducing a third component, and this change affects the membrane morphology (Figure 10).

It is important to stress that many of the aforementioned TIPS solvents are phthalate-based compounds that are considered toxic and harmful to the environment.[29] The membrane industry is now faced with increasingly stringent government regulations, and such toxic solvents need to be replaced in the near future. Recent research, therefore, has focused on identifying potential green and sustainable solvents that provide better performance, or to treat the wastewater generated by the membrane industries.[113]

Cui et al.[106] reported fibrillar PVDF membranes using a green triethylene glycol diacetate (TEGDA) solvent. In contrast to other TIPS-prepared membranes, the highest mechanical strength was obtained using the lowest PVDF concentration. The authors asserted that the interconnected fibrillar morphology gives excellent elasticity (up to 470% strain), which quickly falls to 16% strain on increasing the polymer concentration. This is a very unique type of TIPS structure, and such performances have not been reported before with PVDF polymers (Figure 11). It can be speculated that the conversion from L-L separation to S-L separation caused such drastic performance degradation; but further study is needed to validate and verify the reported results.

Hassankiadeh et al.[29] recently reported a unique solvent for membrane preparation: methyl-5-(dimethylamino)-2-methyl-5-oxopentanoate, which is referred to by the trademark Polar-Clean. This solvent provides many advantages for membrane fabrication. First of all, the solvent is completely biodegradable and environmentally friendly, and is considered to have low toxicity over other solvents. Second, with a similar solubility parameter (21.2 $MPa^{0.5}$) as that of NMP (22.9 $MPa^{0.5}$), it has surprisingly high compatibility with the PVDF polymer (23.2 $MPa^{0.5}$). Also, it is readily available as a commercial product at low cost. Last, the solvent has an extremely high miscibility with water, and a combination of NIPS & TIPS morphologies was observed on membrane fabrication. Such a combined effect is an interesting topic on its own and will be discussed in detail in the following section.

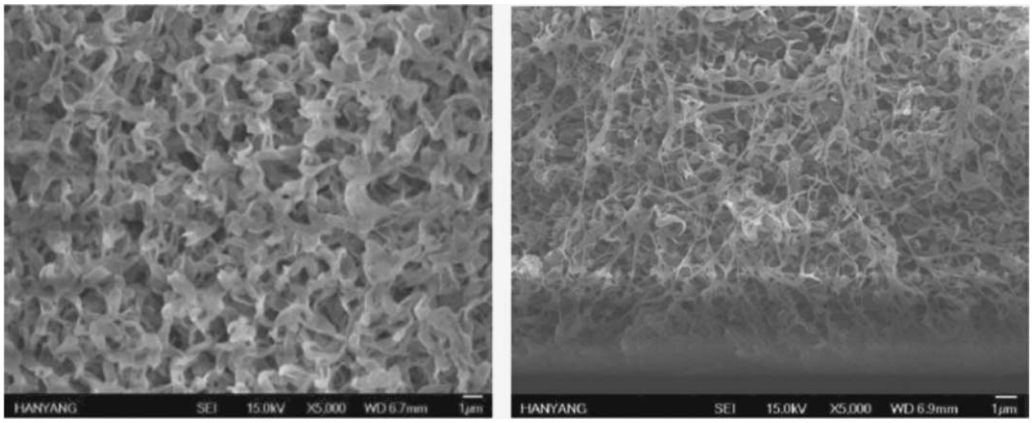

Figure 11. Fibrillar PVDF membranes prepared using 15 wt % PVDF/TEGDA via TIPS.

Such morphology gives excellent elasticity up to 470% due to the interconnected structure.[106]

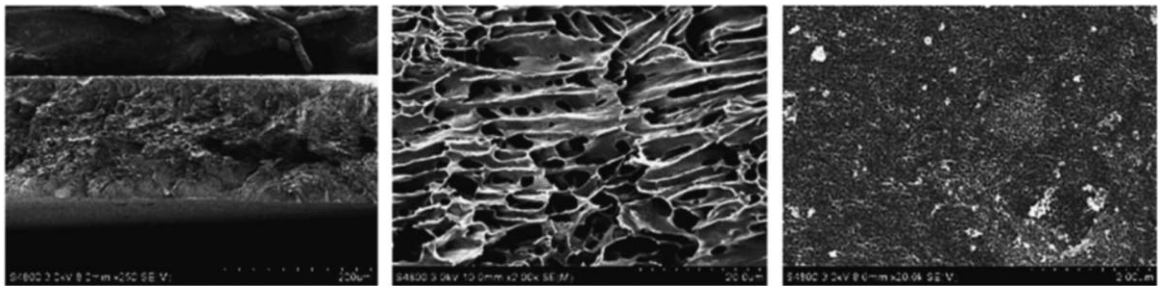

Figure 12. SEM images of 20 wt % PVDF/$DMSO_2$ quenched in a water bath at 30°C to induce liquid-solid separation.[100]

(Left) Full cross section, (center) magnified cross section, and (right) top surface. Tubular pore structures formed due to the use of a crystallizable diluent.

Liang et al.[100] suggested dimethyl sulfone ($DMSO_2$) as a universal crystallizable diluent. $DMSO_2$ is a solid at room temperature and has a molecular weight of 94 Da and a melting point of 106°C. The unique feature of this specific solvent is that it crystallizes near 92°C, resulting in a tubular pore structure on cooling the PVDF/$DMSO_2$ dope solution (Figure 12). This specific case is sometimes referred to as liquid-solid (L-S) separation because the solvent crystallizes within a liquid polymer matrix. Membranes prepared using the L-S separation typically show a tortuous morphology with no significant advantages over other methods; however, recent developments have demonstrated membranes with an aligned pore structure with high porosity and low tortuosity.[114] Liang et al.[100] also developed a diluent recovery protocol using recrystallization and sublimation, making the membrane fabrication more sustainable by minimizing waste. Unfortunately, no polymorphism data were reported; nevertheless, considering the polar nature of $DMSO_2$, β-phase PVDF is expected.

Effect of cooling rate

As explained in the previous section, the polymer–solvent interaction determines the overall macroscopic structure of the prepared membranes (e.g., cellular, fibrillar, tubular, or spherulitic). Conversely, the cooling rate ultimately determines the size of the pores and the size of the spherulites, which affects the overall filtration performance and mechanical integrity of the membranes. More specifically, the effect of cooling rate can be different for L-L phase separation and S-L phase separation (crystallization), as explained in detail below.

The polymer–solvent interaction is a thermodynamic factor, and the cooling rate represents a kinetic factor in the overall membrane formation process. Unlike the polymer–solvent interaction, the effects of the kinetic factor are qualitatively similar for various systems. The prevailing notion in the membrane literature is that the kinetic factor plays the most important role with respect to the membrane performance.

The dope solution cooling rate is mainly a function of the temperature difference between the dope and the cooling environment, ΔT. As mentioned previously, the cooling effect is different for L-L separation and S-L separation. The well-known Nucleation-Growth (NG) model can be applied to describe S-L separation. The NG model suggests that faster cooling rates provide smaller spherulites with smaller pore sizes and higher mechanical strength. Rapid cooling provides many nuclei, but leaves a short time for crystal growth. Conversely, slow cooling provides longer times for growth, resulting in larger spherulites (Figure 13).[85,103,115]

Ghasem et al.,[97] investigated the effect of quenching temperature on TIPS-prepared PVDF HF membranes. As expected, lower quenching temperature decreased the membrane pores and the corresponding water permeability, and vice versa. When the quenching temperature increased from 20 to 35°C, the pore radius increased from 4.47 to 12.86 μm, and the effective surface porosity also increased by a factor of 10. In addition, it was observed that the mechanical strength and the degree of crystallization decreased with increasing bath temperature (decreasing ΔT).

For dope solutions that cross the L-L separation region (below the monotectic point), the pore size is determined by the length of time that the dope stays within the L-L region temperature. For example, longer periods in the L-L phase separation region yield bigger pores with a cellular morphology, as clearly illustrated by Yang et al.,[90] Figure 14. As expected, for dope solutions that do not cross the L-L phase separation region (above the monotectic point), the same cooling procedure did not show a visible difference. Hence, as shown in this work, the cooling procedure can use step protocols (e.g., 1 min in the L-L separation region then quench) to

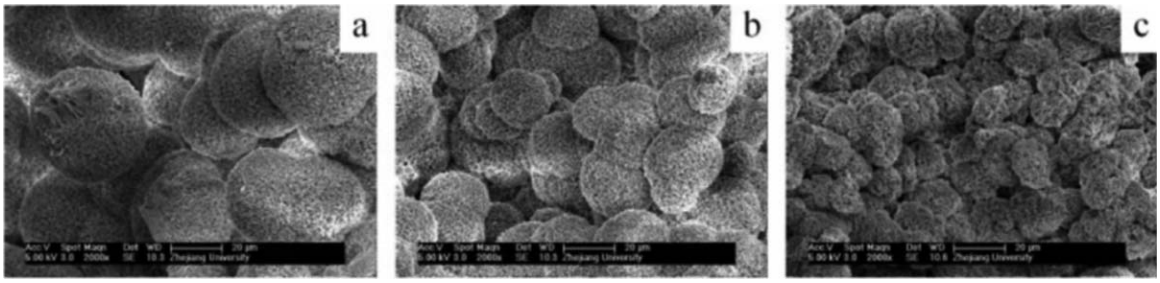

Figure 13. 30 wt % PVDF/DBP membranes cooled at different rates via S-L separation: (a) 5°C min^{-1}, (b) 10°C min^{-1}, (c) 30°C·min^{-1}.[85]

The size of the spherulites increased with slower cooling rates.

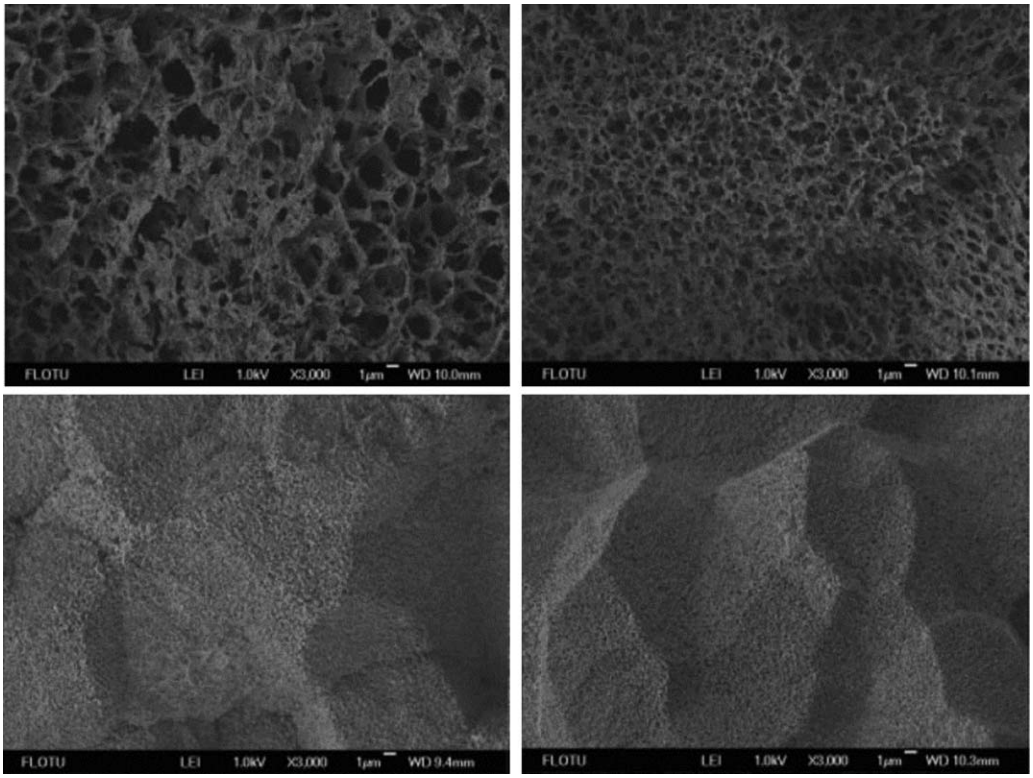

Figure 14. SEM cross-section morphology for TIPS-prepared PVDF membranes.

(Top left) 20 wt % PVDF first cooled to 120°C (L-L separation temperature) for 1 min with subsequent quenching in ice bath; (top right) 20 wt % PVDF immediately quenched to ice bath, shorter residence time in the L-L separation region; (bottom left) 60 wt % PVDF (above the monotectic point) first cooled to 120°C for 1 min with subsequent quenching in ice bath, (bottom right) 60 wt % PVDF (above the monotectic point) immediately quenched to ice bath.

maximize the L-L separation effect. In addition, as noted by Ji et al.,[85] the solution viscosity also affects the phase demixing rate. Unfortunately, the current literature lacks a clear relationship between the L-L separation period and the final membrane performance. Such data would be a valuable addition to the TIPS literature.

As the TIPS diluents are generally extracted after the membrane formation, it is usually assumed that the initial dope composition determines the final membrane porosity.[14] Nevertheless, the rate of cooling has some effect on the porosity. Specifically, faster cooling rates result in membranes with slightly lower porosity compared to the slow-cooled membranes.[103] The cooling rate also affects the polymorphism of the membranes. As this α-phase of PVDF polymer is kinetically favored, increasing the cooling rate generally induces formation of the α-phase over the β-phase.[116]

Effect of additives

The presence of additives or nucleating agents can significantly affect the solution demixing phenomena, ultimately affecting the membrane morphology and performance. For instance, additives can affect the location of the binodal line (thermodynamic effect), or they can initiate or hinder the polymer crystallization (kinetic effect). The overall outcome, however, is very difficult to predict theoretically, and these studies are usually performed empirically.

Additives can affect the membranes in three ways. First, they can act as pore formers to enhance the membrane permeability. Second, they can modify the surface characteristics and make the membranes more hydrophilic or hydrophobic. Finally, additives can improve the membrane mechanical properties. Quite often, more than one effect occurs simultaneously.

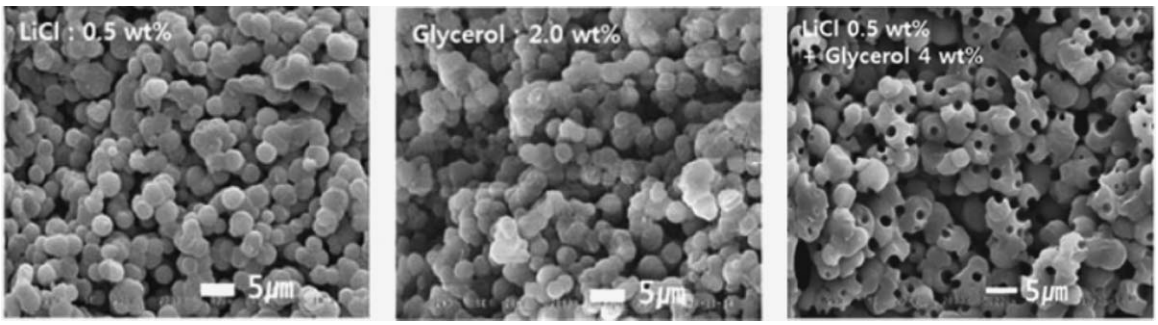

Figure 15. Cross section of 40 wt % PVDF/GBL hollow fiber membranes: (left) with LiCl additive, (middle) with glycerol additive, (right) with LiCl and glycerol additives.

Formation of such fine pores nearly doubled the flux without losing mechanical strength.[28]

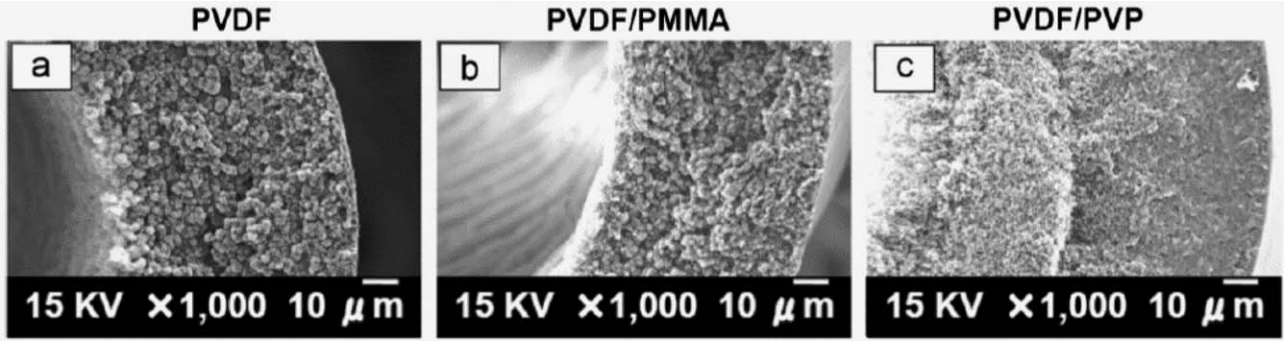

Figure 16. Cross section images of TIPS-prepared PVDF/DEP membranes: (a) 35 wt % PVDF, (b) 25 wt % PVDF/10 wt % PMMA, and (c) 25 wt % PVDF/10 wt % PVP.

Addition of PVP hinders PVDF spherulite formation and induces dense morphology, which decreases the permeability and increases the mechanical strength.[98]

Pore-formers widely used in membrane preparation are polyvinylpyrrolidone (PVP), glycerol, PEG, PMMA, and LiCl. Lee et al.[28] observed formation of fine pores within the spherulites using LiCl and glycerol, as shown in Figure 15. The flux nearly doubled without losing any mechanical integrity. Interestingly, the fine pores did not form when LiCl and glycerol was used separately, but only when they were used together.

Hassankiadeh et al.[29] also used several pore-forming additives to improve the permeability of TIPS-prepared PVDF/PolarClean hollow fiber membranes. Notably, when PVP1300k was used as an additive, the permeability of the membranes increased nearly 1000 times. However, the tensile strength decreased from 6 to 1 MPa, rendering the membranes difficult to handle. Such drastic improvement can be attributed to the formation of surface pores, as PVDF/PolarClean without any additives formed a dense surface layer. This effect (combination of NIPS & TIPS) will be explained in more detail in the subsequent section. The order of additive effectiveness, in terms of permeability, followed PVP > Glycerol > PMMA.

Sometimes the same additive can show completely opposite results. For instance, the use of PVP additives in the work of Cha et al.[83] showed a decrease in permeability with an increase in mechanical strengths for the PVDF/GBL system. The authors attributed this unexpected phenomenon to the swelling of PVP within the pores. Interestingly, the addition of PVP also had a significant effect on the final membrane polymorphism, showing formation of a γ-phase with increasing PVP molecular weight. Rajabzadeh et al.[98] reported a decrease in water permeability with PVP addition in a PVDF/DEP system. In addition, the PVP additive significantly improved the tensile strength (2–7 MPa) and elongation (100–700%) of the membranes. The SEM data revealed that addition of PVP induces formation of a dense layer and hinders formation of PVDF spherulites (Figure 16). Hence, it is speculated that PVP affects the thermodynamic stability of the dope solution and could hinder the kinetics of crystallization depending on the polymer–solvent system. Conversely, addition of PMMA had a negligible effect on the membrane structure and performance.

The use of additives is a simple and convenient method to alter the surface characteristics of the prepared membranes, a common practice in NIPS-prepared membranes. For instance, PVP and PFSA additives are commonly used to make the membranes more hydrophilic.[33] More recently, researchers have been incorporating hydrophobic additives such as nano-

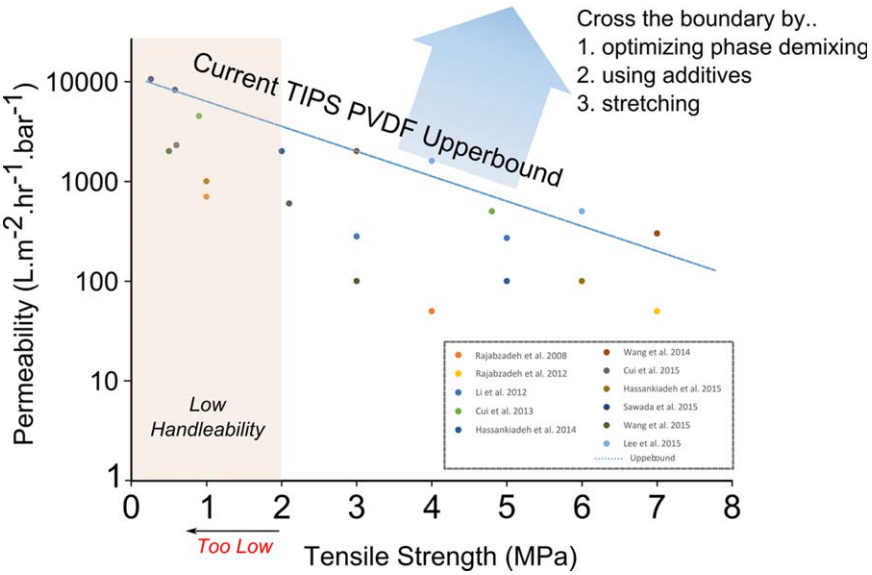

Figure 17. Current permeability upperbound vs. tensile strength for TIPS-prepared PVDF membranes. The upperbound equation is given in Eq. 2.

[Color figure can be viewed in the online issue, which is available at wileyonlinelibrary.com.]

clay[117] and fluorinated silica FSi[118] to make the membranes even more hydrophobic for MD applications. Unfortunately, such research data are rare in TIPS literature, with the notable exception of Cui et al.,[95] who incorporated SiO_2 particles in a PVDF/DBP system and showed improvement in both the water permeability and mechanical strength. Other commonly used additives such as zirconium dioxide (ZrO_2), aluminum oxide (Al_2O_3), titanium dioxide (TiO_2), and graphene and carbon nanotube-based additives could be promising candidates for PVDF TIPS membranes. This is one important topic requiring further research in the TIPS field.

PVDF TIPS membrane performance upper bound

The upperbound concept exists in the gas separation and desalination field, but has not been widely adopted in other membrane fields. This is mainly because it is extremely difficult to compare the membrane performance across membrane, not to mention subjective. Nevertheless, compiling and comparing the TIPS prepared membranes could be quite useful for assessing where the current technology stands at present, and may suggest a direction to focus the future research efforts. TIPS-prepared PVDF membranes, apart from membrane contactors, are commonly used in microfiltration, ultrafiltration, and MBR markets. For such markets, obtaining high mechanical strength and high permeability is important to avoid process failure and to maximize productivity, respectively. These two factors are inversely proportional to each other, that is, increasing mechanical strength exponentially decreases the permeability, and vice versa. It is also important to point out that there is a minimum mechanical strength required (ca. 2 MPa) because it is very difficult to handle the membranes at large scale with mechanical strengths below 2 MPa. Furthermore, fragile membranes may result in process failures from unexpected damage, a risk that industries are reluctant to take. Taking these factors into account, we propose an arbitrary upperbound (Figure 17) for TIPS-prepared PVDF membranes, combining the literature data from the past 10 years (2006–2015)

$$\text{Permeability}\ \left[\text{L.m}^{-2}.\text{h}^{-1}.\text{bar}^{-1}\right] = 11219e^{-0.575\times\text{Tensile Strength [MPa]}} \quad (2)$$

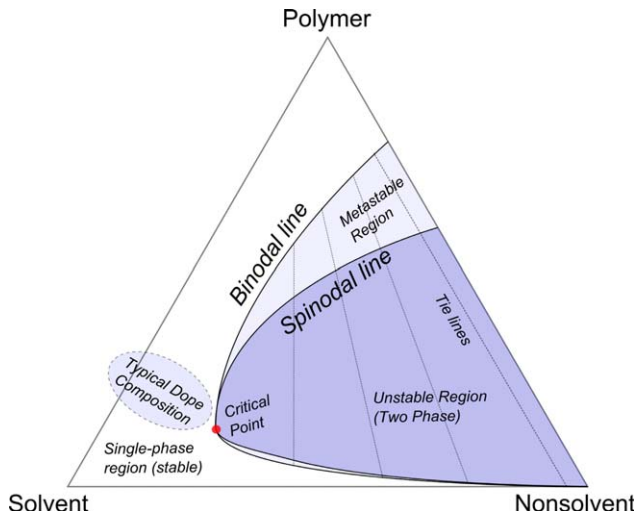

Figure 18. Three component NIPS phase diagram.

[Color figure can be viewed in the online issue, which is available at wileyonlinelibrary.com.]

There are several different approaches to overcome the upperbound. First, the phase demixing mechanism can be fine-tuned to optimize the mechanical strength and permeability. Second, the hydrophilicity of the membranes can be enhanced using additives. There are also many hydrophilization methods that can be used to improve the membrane permeability such as surface coating or grafting.[33] However, it should be noted that hydrophilization is not usually preferred for membrane contactor applications. Third, nanocomposite membranes can be prepared using TIPS by incorporating inorganic particles to improve the mechanical strengths. Finally, post-treatment such as stretching could be used to modify the pore size and porosity of the nascent membranes.

Nonsolvent induced phase separation

NIPS, also known as the Loeb-Sourirajan process, is by far the dominant method used to fabricate polymeric membranes, and it is already well described in other review articles and textbooks[14,27,31,33,66,67]. To prepare membranes by the NIPS method, a dope solution is first prepared by dissolving a polymer of interest in a suitable solvent to form a homogeneous dope solution. The dope solution is then cast as a thin film and subsequently immersed in a nonsolvent bath (e.g., water) to induce polymer precipitation. As compared to the TIPS system, NIPS is more complicated as it is a three component system comprised of a polymer, a solvent, and a nonsolvent. Early works have conceptualized the NIPS process using a three component phase diagram, as shown in Figure 18, to rationalize the precipitation kinetics.[119–121]

In the field of membrane science, NIPS has been intensely researched, and we now have a deep understanding of the membrane formation mechanism and can also control the overall membrane morphology, particularly the skin layer morphology. As the membrane must exhibit a desired separation performance while maintaining flux, the formation of an appropriate skin layer has been the main subject of interest among

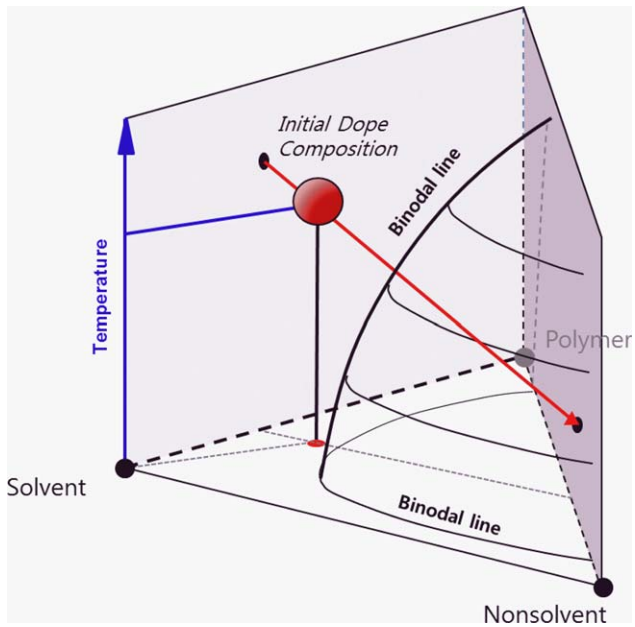

Figure 19. Three-dimensional Phase diagram for the combination of NIPS and TIPS.

[Color figure can be viewed in the online issue, which is available at wileyonlinelibrary.com.]

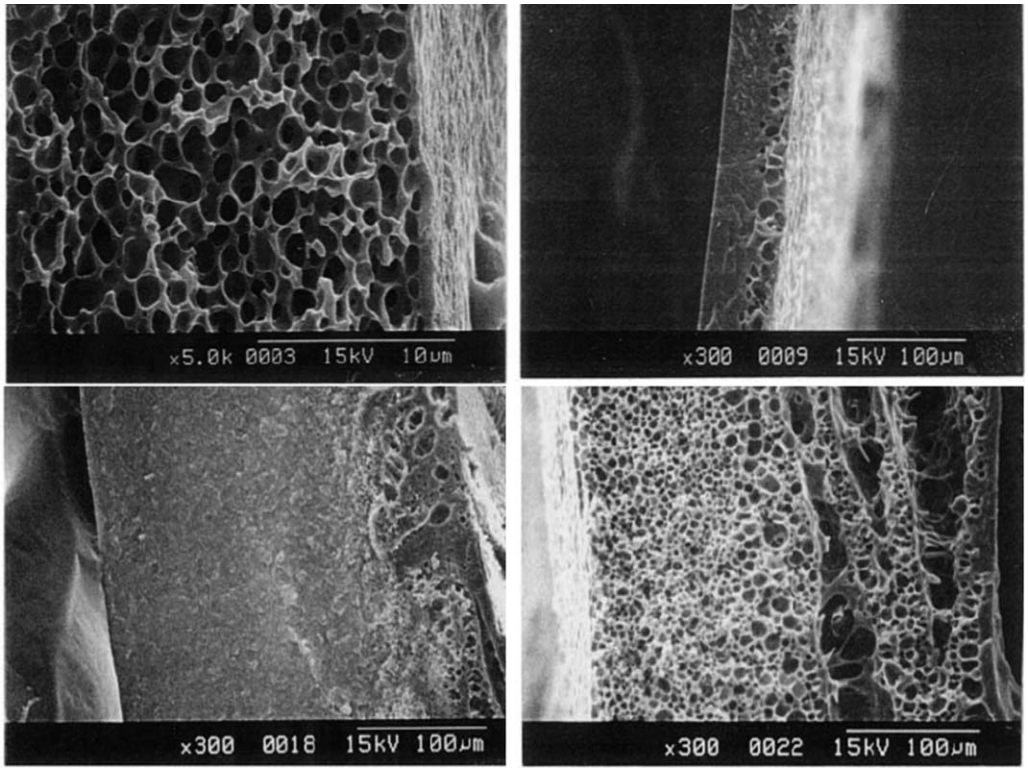

Figure 20. Membranes prepared using PMMA/cyclohexanone system: (top left) via TIPS method, showing cellular morphology, (top right) via NIPS method, showing typical asymmetric morphology, (bottom left) combined NIPS-TIPS after 1 min, (bottom right) combined NIPS-TIPS after 24 h.[129]

membrane researchers. Similar to the TIPS method described before, the effects of solvent,[122] evaporation time prior to immersion,[123] coagulation bath composition and temperature,[124,125] and additives[126] can all be theoretically related to the solution thermodynamics and kinetics of the demixing process. Data now suggest that the membrane formation mechanism is more influenced by kinetics and mass transfer. Nevertheless, manipulating the aforementioned parameters can affect the thickness of the skin layer, pore size, porosity, tortuosity, macrovoids, and ultimately the membrane performance.

As mentioned previously, although there is a convincing theoretical foundation to explain the effect of parameters on the final membrane morphology, it is still very difficult to predict the phase inversion outcome precisely. The current practice to optimize membrane performance is largely empirical using a heuristic approach. PVDF is the main fluoropolymer used in the NIPS process. It is important to note that because PVDF is a semicrystalline polymer, the phase separation behavior is quite different[127] compared to amorphous polymers such as polysulfone and polyethersulfone.[128] Readers are referred to recent thorough reviews on the NIPS method.[31,33]

Combination of NIPS and TIPS (N-TIPS)

In practice, both NIPS and TIPS effect can occasionally take place simultaneously. When the quenching media for the TIPS process is miscible with the TIPS solvent, the NIPS effect can also take place on quenching of the dope solution (Figure 19). As a common example, water is often used as a quenching media for hollow fiber preparation and some TIPS solvents, for example, GBL[28] or Polarclean,[29] have high

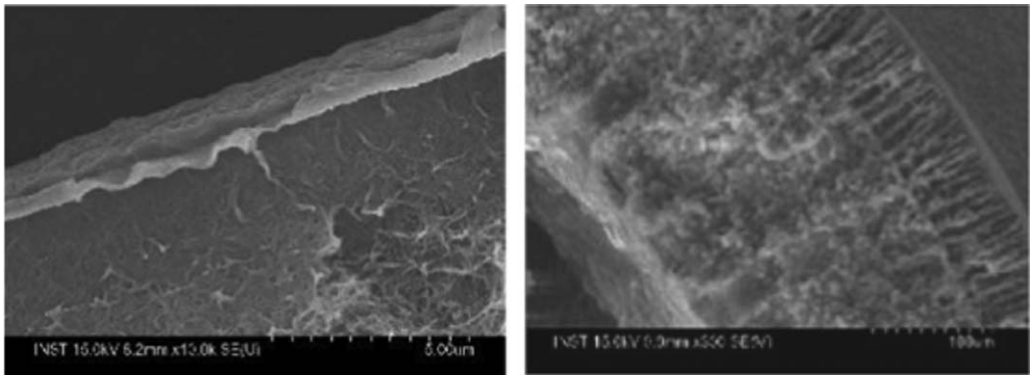

Figure 21. PVDF membranes prepared using PolarClean solvent. (Left) PolarClean's high miscibility with water induced a dense skin layer, and (right) PVP55k additive induced NIPS instantaneous demixing on the surface and created surface pores.[29]

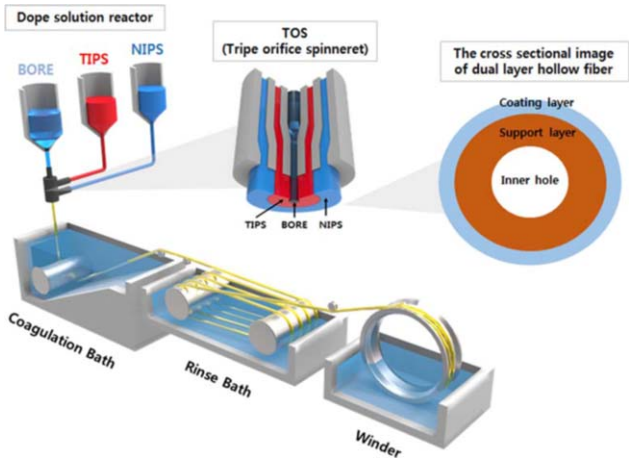

Figure 22. Combination of NIPS and TIPS apparatus.[28]

[Color figure can be viewed in the online issue, which is available at wileyonlinelibrary.com.]

miscibility with water. One may expect that the NIPS effect can occur on the surface of the membrane while the TIPS effect dominates on the support side. The rate of mass transfer, which determines the NIPS morphology, is affected by the system temperature, which also affects the polymer solidification kinetics as well as the surface polymer concentration. Not surprisingly, the system can be further complicated by the use of semicrystalline polymers such as PVDF and ECTFE. This is an area with very limited research, and researchers have often overlooked the NIPS effect for TIPS-prepared membranes quenched in water. Recently, several researchers have identified and exploited such an effect to prepare interesting membranes.

Matsuyama et al.[129] performed an innovative research to isolate the NIPS and TIPS effect and also investigated the combined effect. Using two different coagulation bath media, that is, water and methanol, it was possible control the rate of TIPS and NIPS effects independently. The solvent-nonsolvent diffusion rate affected the polymer concentration, which in

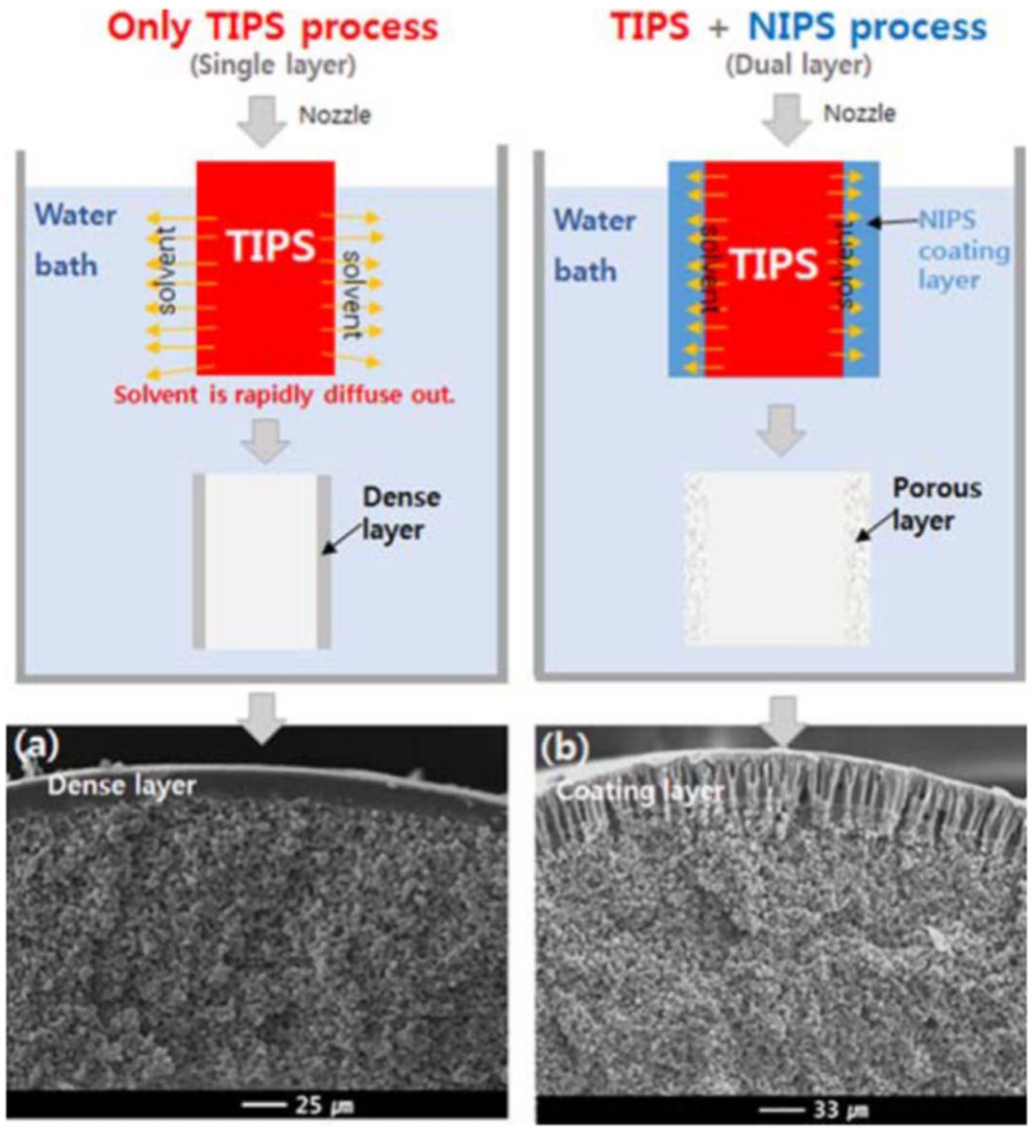

Figure 23. Schematic representation and SEM photos of NIPS-TIPS combined hollow fiber.

Formation of dense skin layer is avoided by coating the surface with a separate NIPS layer that forms a highly porous surface.[28]
[Color figure can be viewed in the online issue, which is available at wileyonlinelibrary.com.]

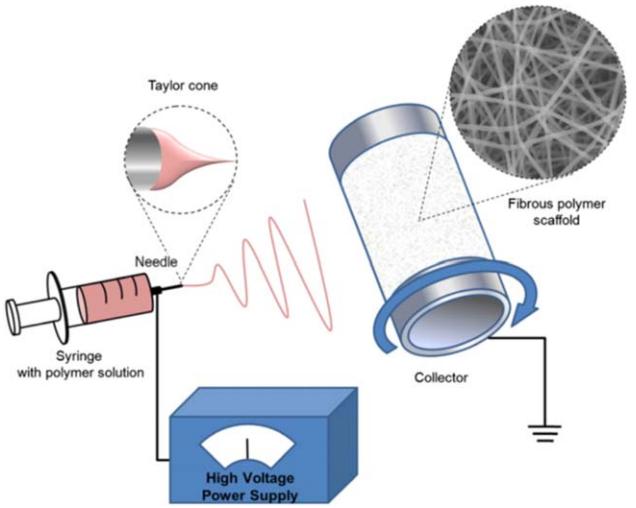

Figure 24. The principle of the electrospinning process.[133]

[Color figure can be viewed in the online issue, which is available at wileyonlinelibrary.com.]

turn shaped the final membrane morphology (Figure 20). Therefore, the immersion time and the nonsolvent media are the critical factors that must be controlled.

Hassankiadeh et al.[29] recently proposed a water soluble green diluent, PolarClean, as a new TIPS solvent. PolarClean exhibited excellent compatibility with PVDF over a wide concentration and temperature range. However, due to the high miscibility of PolarClean with water (quenching bath), fast PolarClean outflow relative to the water inflow resulted in the formation of a dense skin layer with low flux. The effects of quenching bath temperature and dope temperature were analyzed in detail and showed an intricate relationship between the rate of diffusion, heat transfer, and crystallization kinetics and the final membrane morphology. Using different pore-forming additives such as PVP, PMMA, and glycerol affected the NIPS phase demixing rate and created surface pores, which improved the overall membrane permeability, as shown in Figure 21. More specifically, PVP additive moved the initial dope solution thermodynamic state closer to the NIPS binodal line, inducing instantaneous phase demixing to form surface pores.

Cha et al.[130] reported a modified TIPS process (PVDF/GBL system) by changing the quenching media. Changing the DMAc/EG content in the quenching media influenced the NIPS effect between the γ-butyrolactone and nonsolvent, which affected the final membrane morphology. Specifically, increasing the DMAc concentration in the nonsolvent increased the mean pore size and the flux of the prepared membranes. This effect can be readily explained from the NIPS perspective. Increasing the DMAc content in the quenching media reduces the surface polymer concentration, which increases the mean pore size and the flux.

Charged PVDF membranes were fabricated using the TIPS method with PFSA as an additive.[107] Twelve different membranes were prepared with different PVDF-PFSA-NMP ratios at temperatures between 60 and 150°C. However, although the authors claim the membranes were prepared using combined NIPS-TIPS methods, PVDF is highly compatible with NMP solvent and the resulting membranes seem to have formed due to the NIPS effect. This occurs when the crystallization temperature or phase-demixing temperature is located *below* the coagulation bath temperature (25°C in this work). Hence, to understand the true phase inversion behavior, it is important to first obtain a phase diagram, especially for the TIPS process.

A fascinating work by Lee et al.[28] fabricated dual-layer hollow fiber membranes using a triple spinneret (Figure 22). DMAc, a water-miscible solvent, was used as the TIPS solvent, which promoted a NIPS effect on the surface, forming a dense skin layer (Figure 23). However, when a separate dope solution containing pore-forming PVP was used as a coating layer, the surface porosity could be separately controlled. This work, in principle, is similar to the PolarClean work except that two separate dope solutions were used. The support layer assumed a TIPS morphology, whereas the coating layer clearly shows a porous NIPS morphology (Figure 23). Such a design overcomes one of the main limitations of the TIPS hollow fiber membranes, which form a dense skin layer when the solvent has miscibility with water.

A recent work by Xiao et al.[131] fully exploited the NTIPS method to prepare high performance MD membranes with high porosity and high liquid entry pressure using a PVDF/ε-caprolactam system. The membrane properties and the MD performance reported in this work are impressive relative to the commercial PVDF membranes: the reported porosities were 79–96%, liquid entry pressure values were 3.5–8 bar, and MD flux reached as high as 85 kg m^{-2} h^{-1} at 80°C feed temperature.

The N-TIPS method was recently studied theoretically using the dissipative particle dynamics simulation by Tang et al.[112] which confirmed the effects of coagulation bath temperature and the polymer–solvent interaction on skin formation kinetics.

Having the NIPS effect in TIPS-prepared membranes may seem like a disadvantage, and it does complicate the process. However, if NIPS and TIPS effects can both be controlled separately, similar to the thin-film composite membranes, which now dominates the RO market, the surface morphology can be further fine-tuned to improve both the porosity and flux without sacrificing the narrow pore size distribution.

Electrospinning Method

Electrospinning is one of the fabrication methods used to prepare highly porous membranes with high porosity, high surface area, and excellent pore interconnectivity, and it has been actively researched for various applications in tissue engineering, sensor materials, piezoelectric nano-generators, lithium ion battery separators, and membrane applications.[132] Although the method still suffers from several drawbacks such as low scalability, low productivity, and difficulty in fabricating sub-100 nm pores, the electrospinning method offers excellent advantages for membrane contactor applications such as high surface porosity, high hydrophobicity, and low tortuosity. A typical electrospinning apparatus consists of a high voltage supplier, a polymer solution feed system, and one or more collectors. When an electric potential higher than the surface tension of the polymer solution is applied, the polymer solution ejects from the nozzle to the collector as a conically shaped nanofiber (Taylor cone), as illustrated in Figure 24. During the flight from the nozzle to the collector, most of the solvent is evaporated, leaving the dry nanofibers to stack and form an electrospun membrane.

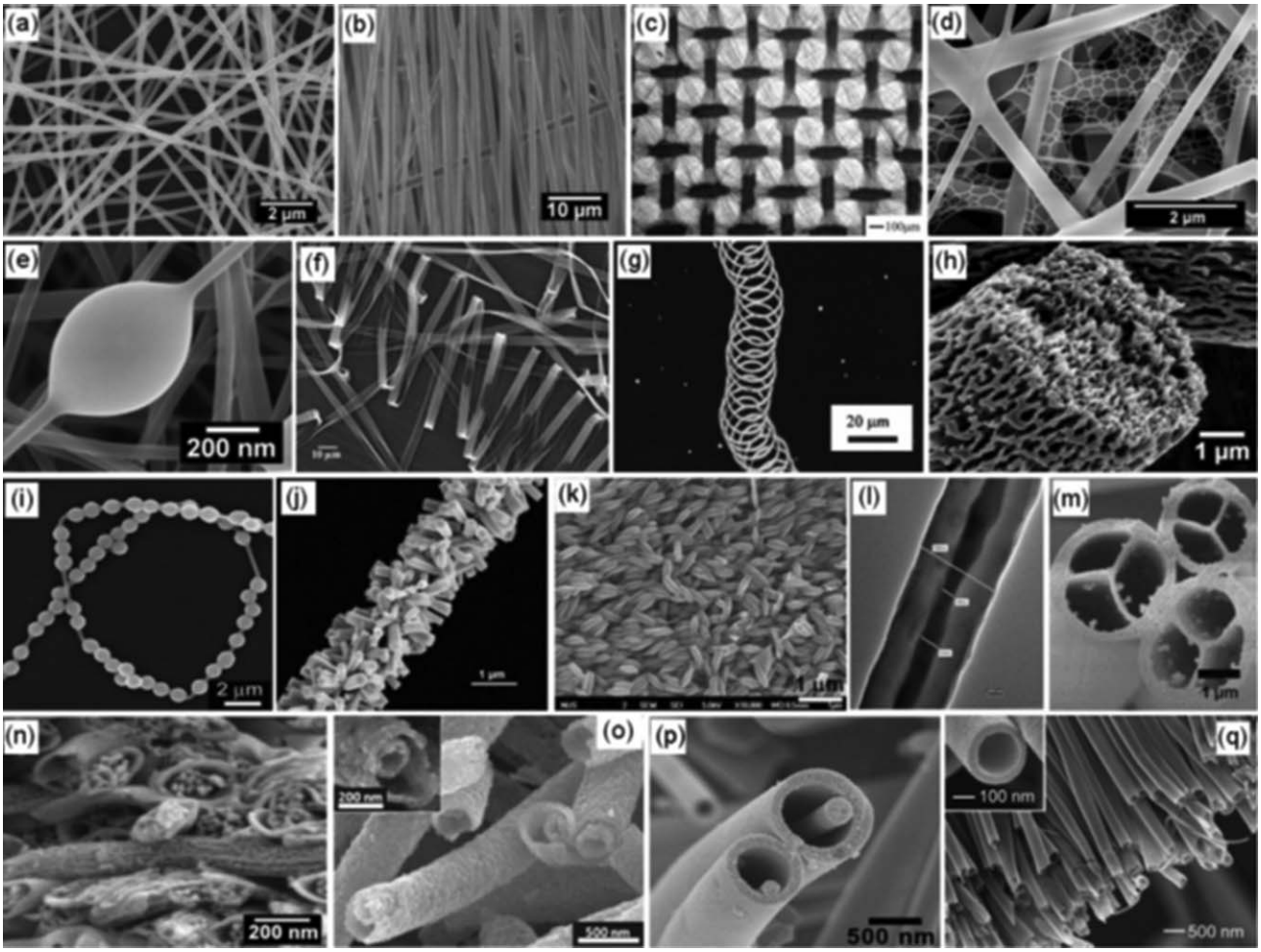

Figure 25. Different types of nanofibers fabricated by electrospinning compiled by Wang et al.[134]: (a) random oriented, (b) aligned, (c) patterned, (d) spider-web-shaped, (e) beading, (f) ribbon-like, (g) helical, (h) porous, (i) necklace-like, (j) firecracker-shaped, (k) rice grain-shaped, (l) core-shell, (m) multichannel tubular and (n) multicore cable-like nanofibers, (o) tube in tube, (p) nanowire in microtube and (q) hollow structures.

As summarized in Figure 25, various types of microstructures can be fabricated for different applications using electrospinning.[134] The nanofiber morphology can be controlled by changing processing conditions and the shapes of the needle and collector; therefore, understanding the influence of each factor is important to tailor the nanofiber morphology for the desired application.

There are several different kinds of electrospinning systems with different types of needle shapes and collectors,[135] and each type of needle and collector can control the nanofiber

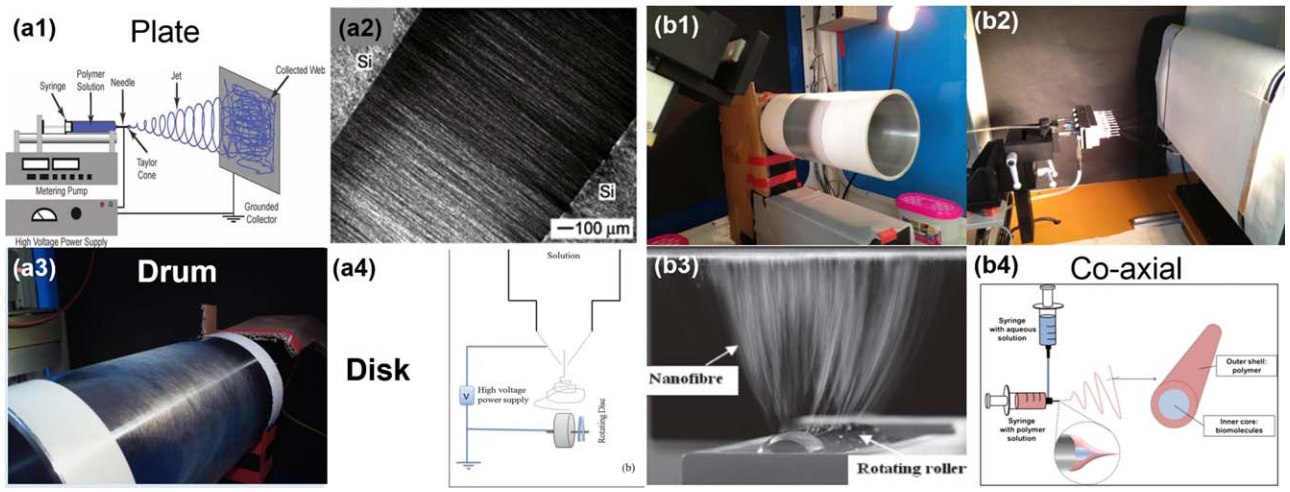

Figure 26. Various types of needles and collectors for the electrospinning process.[133,135–137]

[Color figure can be viewed in the online issue, which is available at wileyonlinelibrary.com.]

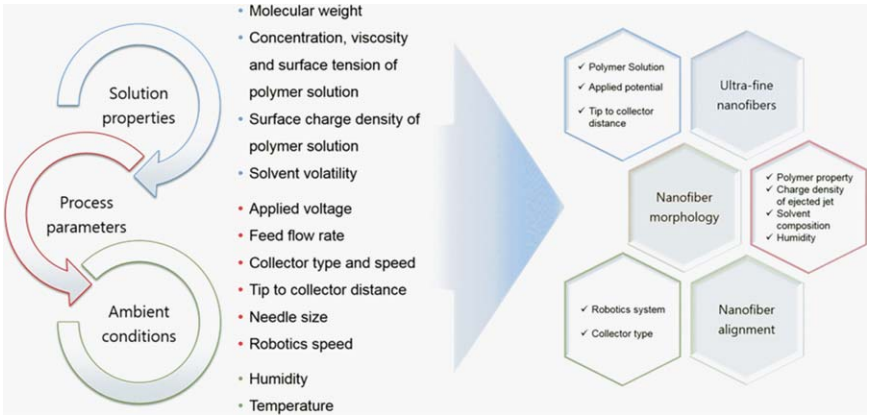

Figure 27. Classification of main parameters influencing the electrospinning process.

[Color figure can be viewed in the online issue, which is available at wileyonlinelibrary.com.]

morphology and alignment in different ways, as shown in Figure 26.

Among the different collectors, the plate-type collector is the most widely used due to its simplicity and versatility. Fibers can be spun close to the collector, and the fibers can be patterned by moving the needle and collector. Also, the electrospun fibers can be aligned using drum-type, disc-type, and counter electrode array-type collectors. Although the disc-type collector and the counter electrode array-type collector can be used to fabricate highly aligned fibers, it is difficult to scale-up these techniques. Conversely, the drum-type collector can be used to fabricate large area electrospun membranes with sufficient nanofiber alignment.

The single nozzles are most widely used for lab-scale electrospinning experiments. For larger scale production, multinozzle and needleless types of electrospinning processes are available. The multinozzle system is relatively simple and easily scalable due to the nozzle modularity. Conversely, needleless electrospinning can produce an electrospun membrane at high rate, but the diameter distribution of the electrospun nanofiber is broader than that of others.[138] Recently, co-axial nozzles have been developed to fabricate hollow nanofibers.[139]

To tailor electrospun membranes for various applications, one needs a thorough understanding of the effects of different parameters. Although there are many different parameters that can be controlled in electrospinning, some of the key parameters which significantly influence the nanofiber morphology have been clearly demonstrated in the literature.[132] As illustrated in Figure 27, the key factors can be classified into process parameters, solution properties, and ambient conditions.

As mentioned previously, the prerequisite for electrospinning is overcoming the surface tension of the polymer solution by applying sufficient electrical potential. The required applied potential (V_c) can be calculated using Eq. 3[140]

$$V_c^2 = 4\left(\frac{H^2}{L^2}\right)\left(\ln\frac{2L}{R} - 1.5\right)(0.117\pi R\gamma) \tag{3}$$

where H (cm) is the tip-to-collector distance, L (cm) is the nozzle length, R (cm) is the radius of the nozzle and γ (dyn/cm) is the surface tension of the polymer solution.

In this review, we discuss the effects of concentration, the viscosity of the polymer solution, polymer molecular weight, applied potential, tip-to-collector distance, temperature, and humidity, all of which affect the nanofiber morphology. In addition, the control of PVDF polymorphism using the electrospinning method is reviewed.

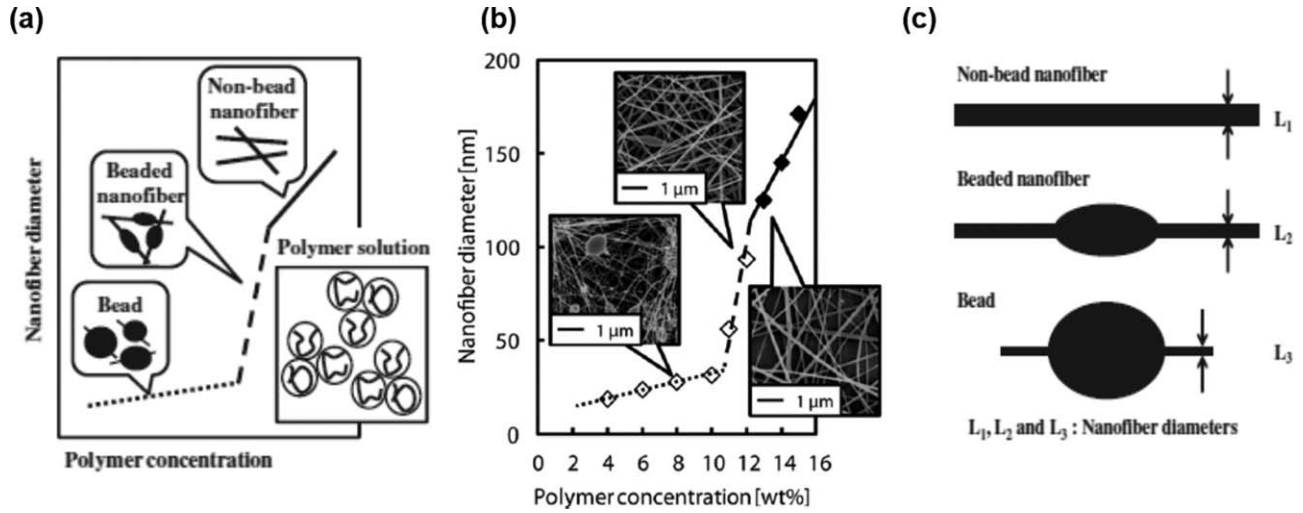

Figure 28. Effect of polymer concentration on the nanofiber morphology: (a) change of nanofiber morphology depending on polymer concentration, (b) SEM images of nanofibers in accordance with polymer concentration, (c) schematic illustrating the change in nanofiber morphology.[141]

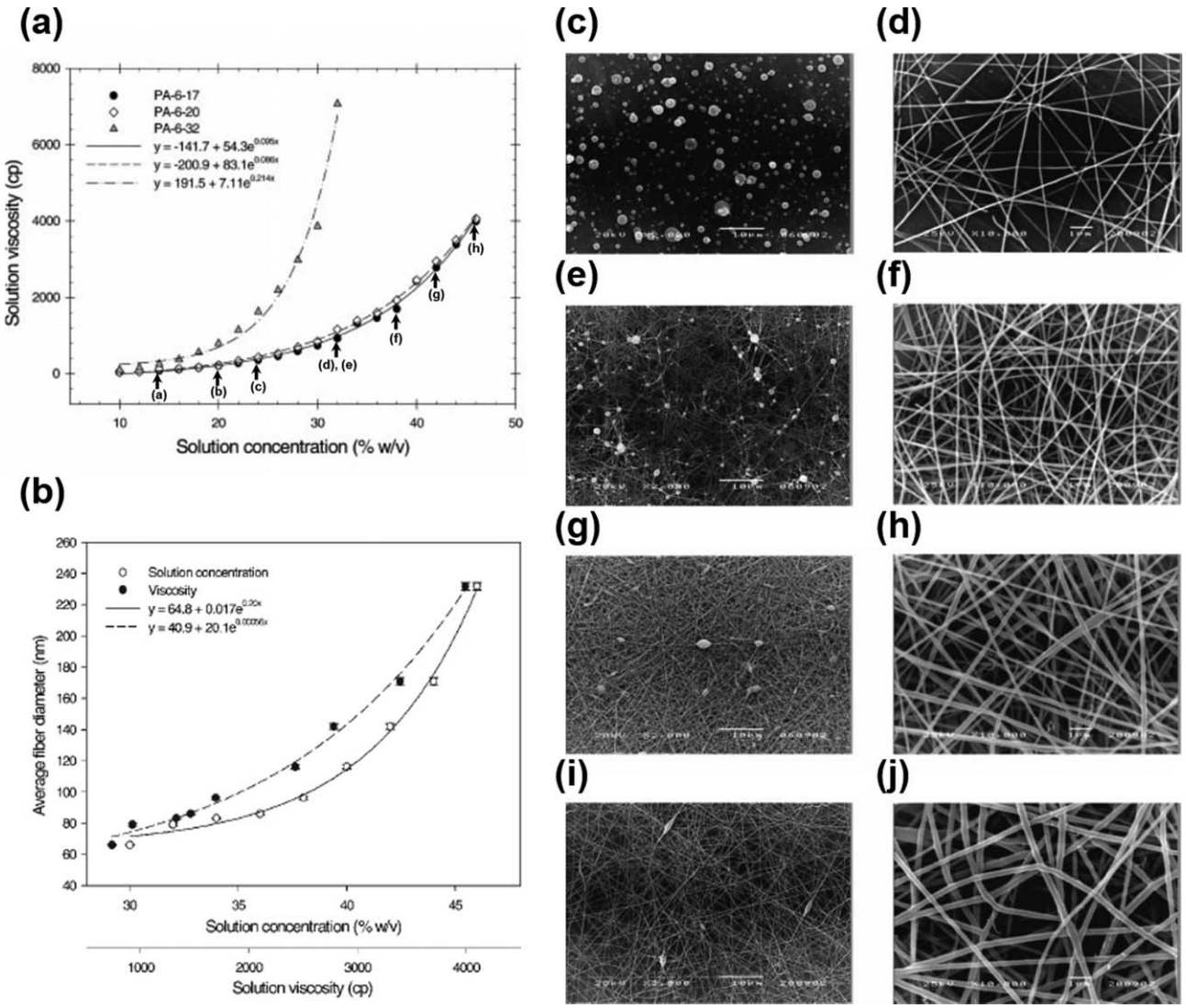

Figure 29. The effect of solution viscosity on polyamide nanofiber morphologies fabricated using different polymer solution concentrations: the solution viscosity vs. solution concentration, and the nanofiber diameter vs. solution concentration.

SEM images of polyamide nanofibers fabricated from different solution concentrations (viscosities): 2k magnified images of (a) 14 wt %, (b) 20 wt %, (c) 24 wt %, and (d) 32 wt %, and 10k magnified images of (e) 32 wt %, (f) 38 wt %, (g) 42 wt %, and (f) 46 wt %.[142]

Effect of polymer solution properties

Concentration of the Polymer Solution. The concentration of the polymer solution is one of the most important parameters to control during electrospinning. Polymer concentration can be manipulated to control the presence of beads and microparticles. As shown in Figure 28, Arai and

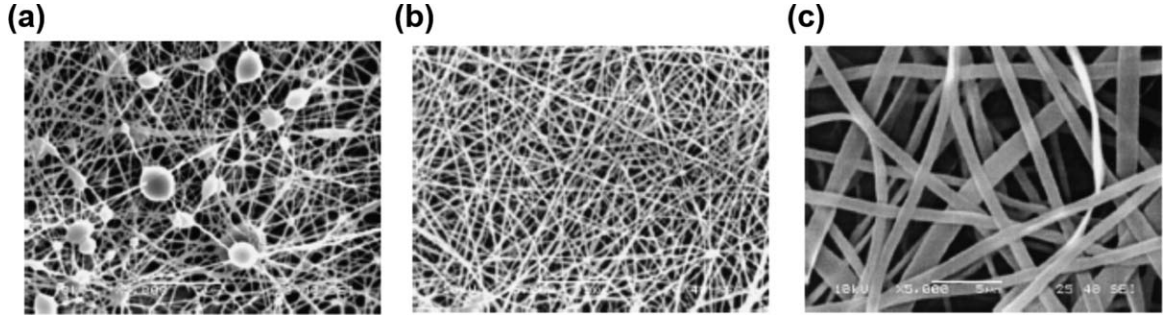

Figure 30. The effect of polymer molecular weight on PVA nanofiber morphology fabricated with PVA of different MWs: 25 wt % polymer solutions of (a) 9000–10,000 Da, (b) 13,000–23,000 Da, and (c) 31,000–50,000 Da PVA.[143]

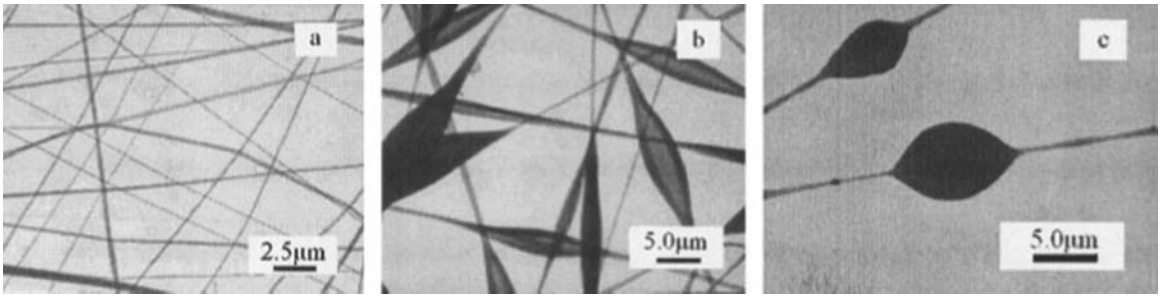

Figure 31. The effect of solvent on PVP nanofibers; TEM images of PVP nanofibers fabricated from 4 wt % (a) EtOH, (b) MC, and (c) DMF solutions.[146]

Kawakami[141] demonstrated that there exists a critical concentration range where the nanofibers are fabricated as an intermediate state between a bead and a nanofiber. At the concentration below the critical region, bead and microparticle morphology dominates in the prepared membranes due to the high surface tension and low viscosity of the polymer solution. Above the critical region, smooth, fine nanofibers can be obtained. If the polymer concentration is much higher than the critical region, a helix-shaped micro-ribbon morphology was observed.[132]

In most applications, ultrafine nanofibers are favored (above the critical region) because the beads or microparticles usually reduce the mechanical strength of the electrospun membranes. Such microstructures are considered as defects. Conversely, beads and microparticles are preferred for membrane contactor applications that favor super-hydrophobicity due to the enhancement of surface roughness.[138]

Viscosity of the Polymer Solution. The viscosity of the polymer solution is proportional to the concentration of the polymer solution. Therefore, the solution viscosity shows a trend similar to that of the polymer concentration in terms of the nanofiber morphology, as summarized in Figure 29. Mituppatham et al.[142] fabricated polyamide (MW 17,000 Da) nanofibers using different polymer concentrations, which have different solution viscosities. When the viscosity was higher than 1332 cP (34 wt % polymer), smooth nanofibers were obtained without beads and microparticles. The authors assert that high polymer concentration implies less solvent for evaporation during the flight, which reduces the bead formation. In addition, high viscosity results in larger fiber diameter due to the lower elongation tendency. As shown Figure 29, the effect of polymer concentration and the solution viscosity on the prepared fibers are similar and can be expressed as an exponential relationship.

Molecular Weight of Polymer. At a fixed polymer concentration, the molecular weight of the polymer determines the entanglement degree of the polymer chains in the solution. Therefore, the polymer molecular weight also affects the nanofiber morphology (Figure 30).[132] Although the solution concentration, viscosity, and polymer molecular weight are closely related to each other, the morphology of the electrospun nanofibers is primarily affected by the solution viscosity and the surface tension of the polymer solution. Nevertheless, smooth nanofibers can be prepared using low molecular weight polymers,[143] hence, a high molecular weight is not always essential for electrospinning. If the molecular weight is low, the polymer concentration should be high enough to provide sufficient intermolecular interactions for formation of electrospun nanofibers. Conversely, if the polymer molecular weight is high, a microribbon-like morphology could be obtained even at low polymer concentrations.[143–145]

Effect of Solvent. The solvent evaporation rate during the flight of the polymer solution is strongly affected by the viscosity and surface tension of the polymer solution. Yang

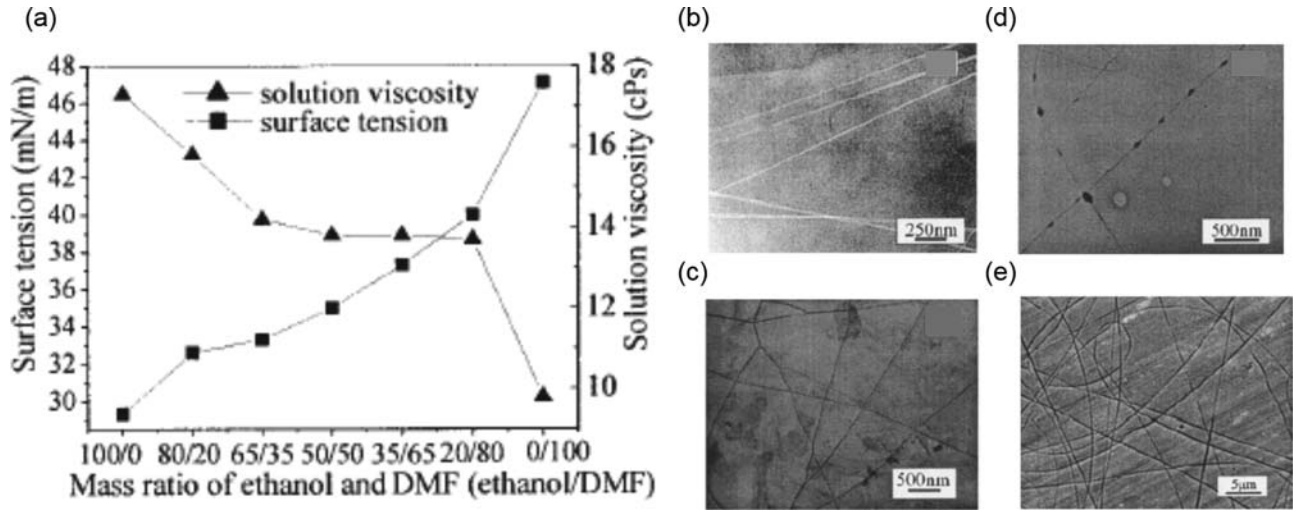

Figure 32. The effect of mixed solvent systems on PVP nanofibers: (a) surface tension and viscosity for different mixed solvent systems.

TEM images of 4 wt % PVP nanofibers from different compositions of EtOH/DMF: (b) 65/35, (c) 50/50, (d) 35/65, and (e) SEM image of 4 wt % PVP nanofibers using EtOH/DMF (50/50).[146]

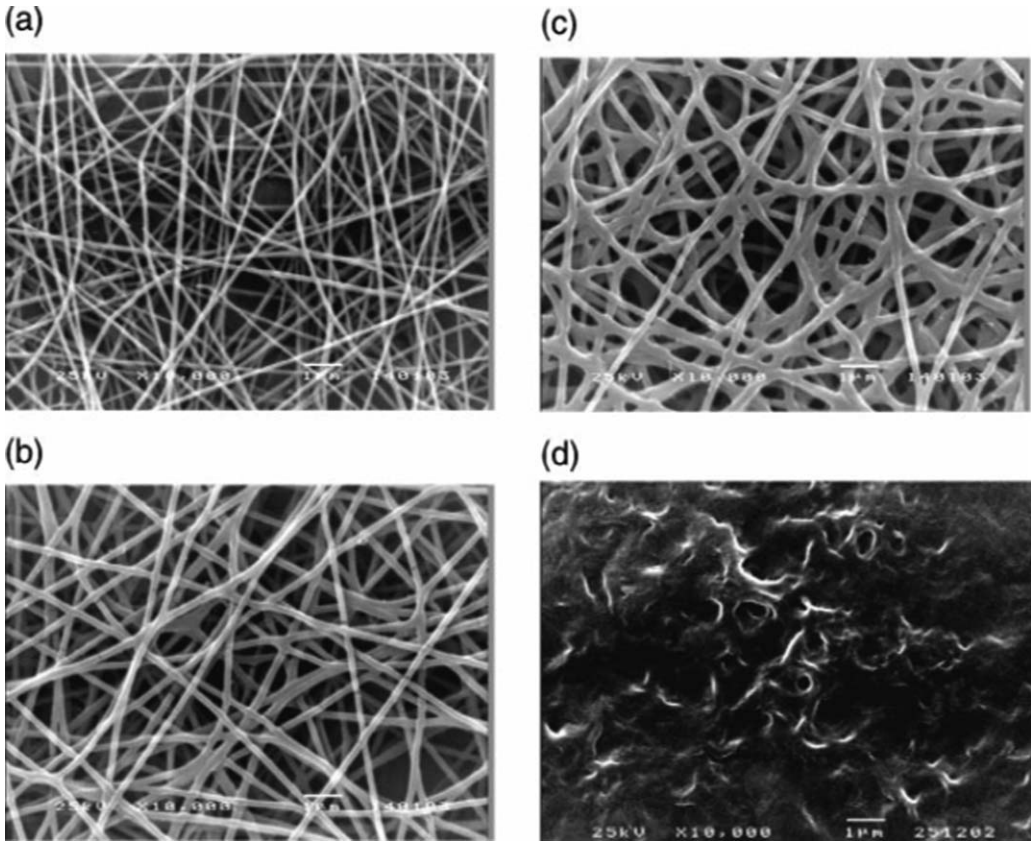

Figure 33. Effect of solvent mixtures on polyamide nanofibers fabricated with different solvent mixtures (formic acid/*m*-cresol): (a) 90/10, (b) 80/20, (c) 60/40, and (d) 0/100.[142]

et al.[146] studied the effect of solvent on PVP nanofibers using different kinds of solvents under the same electrospinning conditions. As shown in Figure 31a, PVP nanofibers from a PVP/EtOH solution resulted in smooth nanofibers without beads. Conversely, PVP nanofibers fabricated from PVP/MC and PVP/DMF solutions showed spindle and sphere-shaped beads, respectively (Figures 31b, c). Such a difference occurs because the PVP/methylene chloride and PVP/DMF solutions have lower surface tension and higher viscosity than those of PVP/EtOH solution. Interestingly, the spindle-shaped bead fabricated from the PVP/MC solution exhibited a hollow fiber morphology induced by the low boiling temperature of MC, which rapidly evaporated on the surface of the ejected jet.

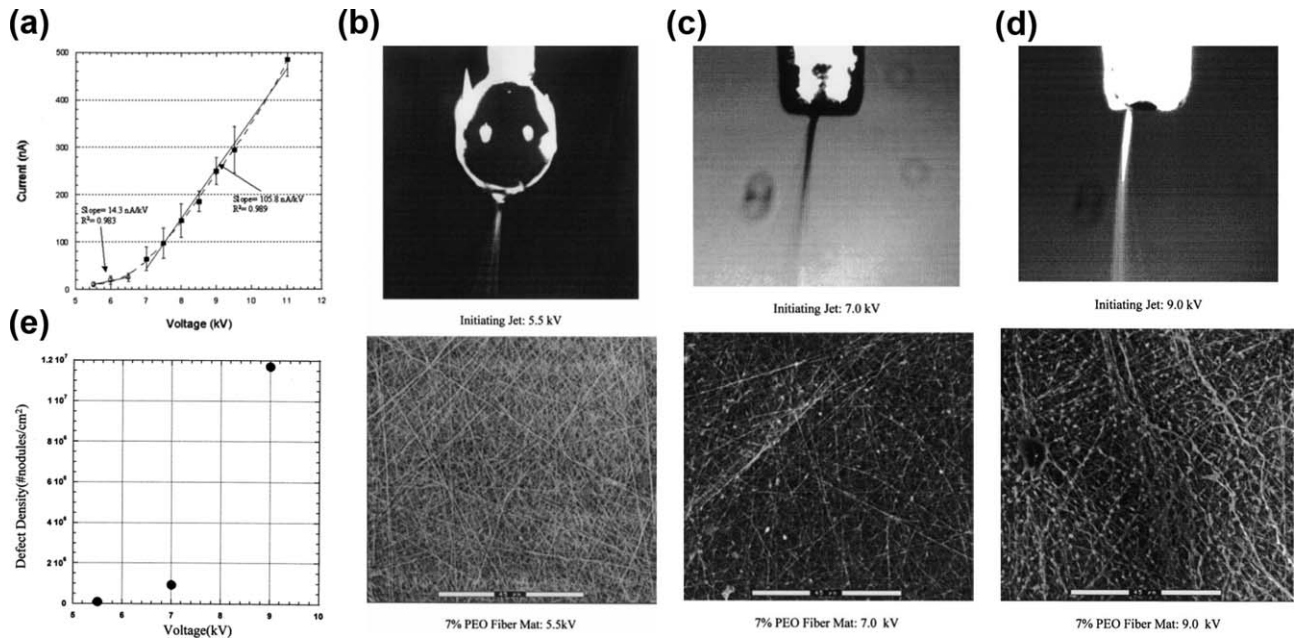

Figure 34. SEM images of PEO nanofibers as a function of applied potential.[150]

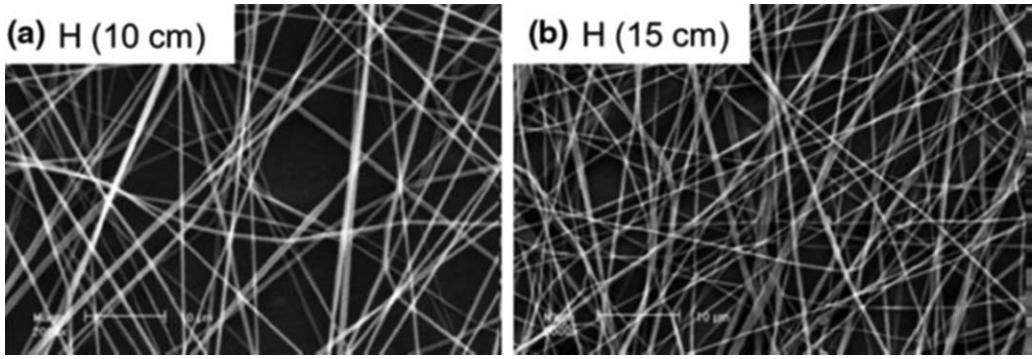

Figure 35. The effect of tip-to-collector distance on the diameter of electrospun nanofibers fabricated using a 20 wt % PS/DMAc solution with 10 kV at (a) 10 cm and (b) 15 cm of tip-to-collector distance.[151]

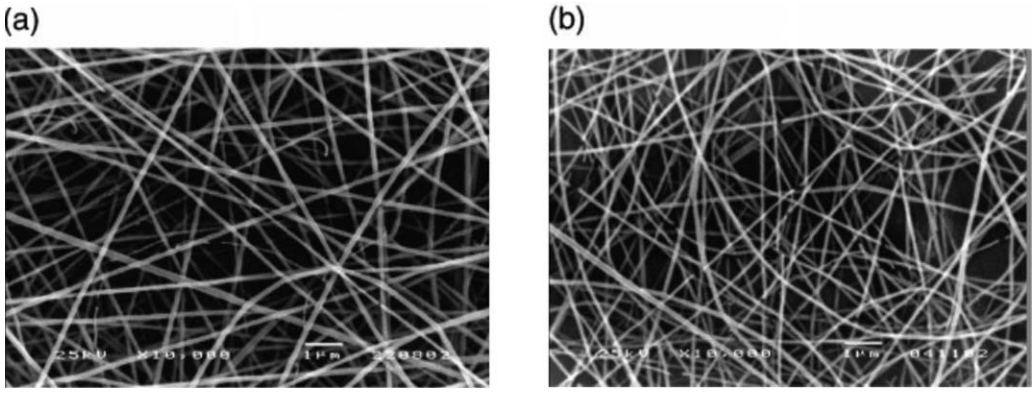

Figure 36. Effect of temperature on the morphology of electrospun PA-6-32 nanofibers, which were fabricated at (a) 30°C and (b) 60°C using 20 wt % of PA-6-32 dissolved in an 85% formic acid solution.[142]

Yang et al.[146] also investigated the effect of mixed solvent systems on nanofiber morphology. As shown in Figure 32, the surface tension and viscosity of the polymer solution showed an inverse relationship. In addition, when the DMF content in the mixed solvent system increased, the resulting nanofiber diameter decreased from 250 nm down to 20 nm and did not show any beading.

Mit-uppatham et al.[142] prepared 32 wt % polyamide (MW 20,000 Da) dissolved in formic acid and *m*-cresol under various compositions. As shown in Figure 33, the fiber diameter increased in accordance with increasing *m*-cresol content, which has a high boiling temperature (202°C) and low dielectric constant (11.5 at 24°C). At 100% *m*-cresol, the polyamide nanofibers eventually fuse together due to the residual solvents.

As mentioned previously, the importance of using greener chemistry in the chemical industry has been growing in accordance with environmental regulations. Although typical solvents like DMF, DMAc, and NMP are commonly used for

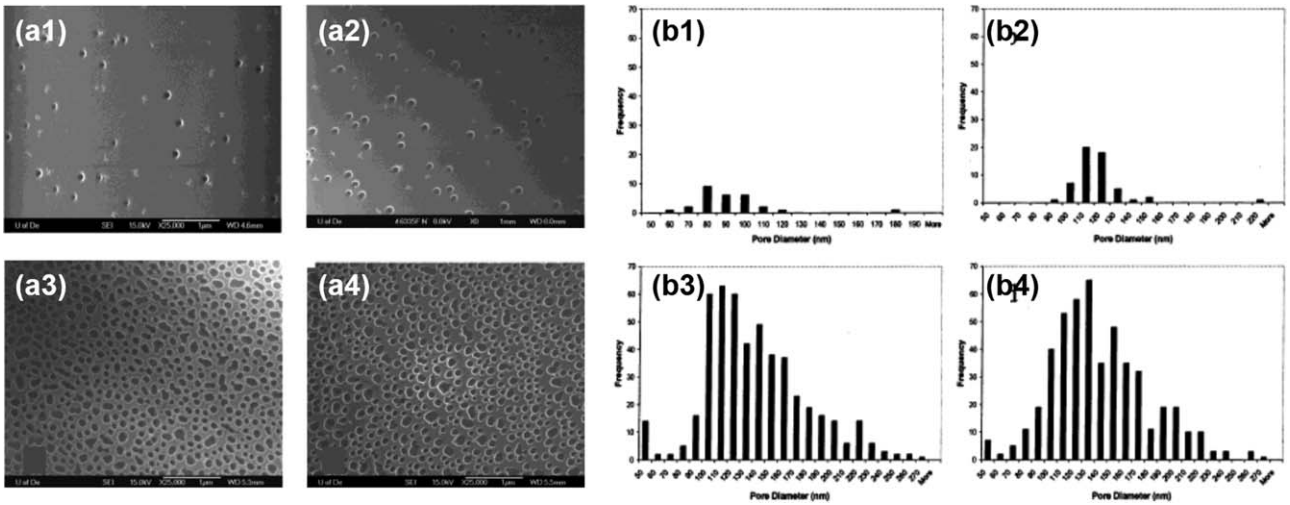

Figure 37. Effect of humidity on morphology of electrospun PS nanofibers fabricated at various humidity conditions; SEM images and pore distribution on the nanofibers at (a1 and b1) 31–38%, (a2 and b2) 40–45%, (a3 and b3) 50–59%, and (a4 and b4) 60–72% humidity.[153]

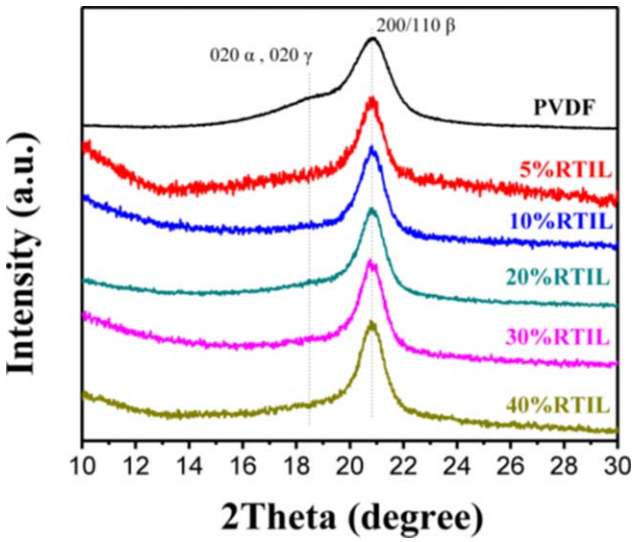

Figure 38. Room-temperature wide angle X-ray scattering intensity ($\lambda = 0.1542$ nm) of electrospun PVDF and PVDF/RTIL composite electrospun membranes at different RTIL compositions.[154]

[Color figure can be viewed in the online issue, which is available at wileyonlinelibrary.com.]

the electrospinning method due to their excellent compatibility with various polymers and high dielectric constant, such solvents must be replaced with greener alternatives. Unfortunately, research on green solvents for electrospinning has not yet been performed.

Effect of processing parameters

Effect of Applied Potential. Generally, higher applied potential produces thinner fibers and smaller beads[147] due to the greater force applied onto the jet that stretches the fiber. In addition, fibers prepared using high applied potential typically show a rough surface morphology.[148] Although debatable, Deitzel et al.[149] reported that if the applied potential becomes too high, the electrospun jet becomes unstable and increases the fiber-bead density. As shown in Figure 34a, when the electric potential increases above 7 kV, the slope of the current curve becomes steeper. In addition, the solution droplet at the end of the needle gets smaller with increasing electric potential, as shown in Figures 34b–d. It can also be seen that the bead density sharply increases above 7 kV (Figure 34e). However, it should be pointed out that there is as yet no consensus among researchers on how the applied potential influences the nanofiber morphology. Therefore, the applied potential should be optimized depending on the polymer properties, solution concentration, and tip-to-collector distance to fine-tune the morphology of the electrospun nanofibers.

Effect of Tip-to-Collector Distance. The distance from the tip of the needle to the collector should be long enough for solvent evaporation and polymer solidification. If the distance is too short, the polymer may not fully solidify, which would decrease the final membrane porosity. Conversely, if the distance is too long, beads could form on the fibers because the applied potential cannot provide enough elongation force to stretch the polymer solution, as described in Eq. 3. Hence, there exists an optimum tip-to-collector distance for each polymer dope solution. Yuan et al.[151] observed that longer distances produces thinner nanofibers using a 20 wt % PSF/DMAc solution at 10 kV. As clearly shown in Figure 35, when the tip-to-collector distance is changed from 10 to 15 cm, the fiber diameter decreased from 438 ± 72 nm to 368 ± 59 nm.

Effect of ambient conditions

Effect of Temperature. As the solution viscosity is inversely proportional to the temperature, higher temperatures result in thinner fibers and/or beaded fibers.[132] For example, Figure 36 shows a decrease in fiber diameter when the temperature increased from 30 to 60°C. Interestingly, it can also be seen that the fiber density also increased with temperature, compensating for the decrease in fiber diameter.

Effect of Humidity. The humidity has significant influence on the rate of solvent evaporation, which in turn affects the surface morphology of the electrospun nanofibers.[152] Casper et al.[153] demonstrated that the number of pores and pore size on the surface of polysulfone nanofibers increased as the humidity increased, as shown in Figure 37. The effect is more drastic in the lower humidity range (31–45% humidity) with no visible difference in fiber morphology above 59% humidity. Conversely, the pore size distribution became broader with increasing humidity.

Controlling the PVDF Polymorphism. PVDF polymer is one of the most widely used material for electrospinning because it can be used to form thin membranes with high specific surface area and high porosity. In addition, PVDF has good mechanical properties and is highly resistant to heat, abrasion, and chemicals. Membranes with extremely high β-phase content (50–100%) have been reported in the PVDF electrospinning literature.[154–156] The electrospinning method intrinsically favors β-phase formation for two reasons. First, the method requires a polar solvent with a high dielectric constant for spinning. Second, the applied potential induces uniaxial stretching via electrical poling. As a result, the dipoles in the electrospun PVDF (CF_2 and CH_2 dipoles) nanofibers become oriented, which favors the formation of a β-phase.[154] The spinning parameters significantly influence the PVDF

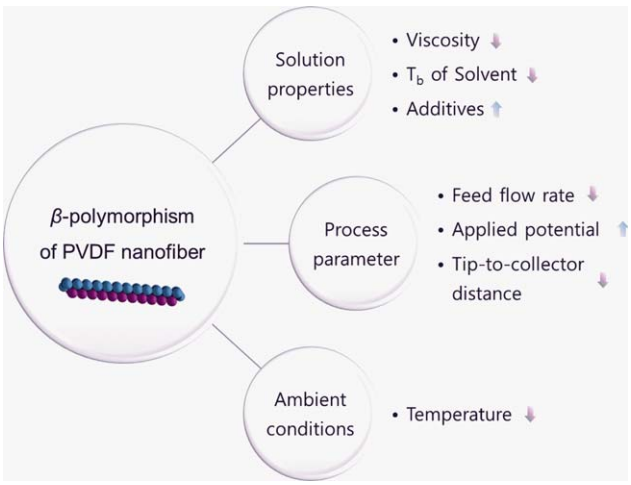

Figure 39. Summary of the electrospinning parameters to induce PVDF β-phase formation: low viscosity,[163] low boiling point solvent,[156] high additive content,[155,162] low feed rate,[156] high applied potential,[163] short tip-to-collector distance,[156] and low ambient temperature (<90°C).[163]

[Color figure can be viewed in the online issue, which is available at wileyonlinelibrary.com.]

polymorphism in electrospun membranes. Zheng et al.[156] investigated spinning parameters for β-polymorphism formation such as the solvent composition, temperature, feeding rate, and tip-to-collector distance. Typically, the β-phase content in the electrospun PVDF membranes are above 80% in the literature.[155]

Apart from the spinning parameters, partially charged additives have been studied for β-phase formation in the PVDF research using various kinds of additives such as nanosilicates[157,158] and carbon nanotubes.[159–161] Interactions between the partially positive hydrogen atoms in the PVDF chain and the partially negative additives like fluorine-based fillers[155,162] and between the partially negative CF_2 group in the PVDF chain and partially positive additives[154,162] can be exploited to control the β-phase content. For instance, it has been shown that PVDF electrospun membranes containing partially charged additives exhibited higher β-phase content than that of nascent PVDF electrospun membranes [154,155]. Recently, Xing et al.[154] prepared 100% β-phase PVDF membranes using a blend of PVDF and room-temperature ionic liquid (RTIL). As shown in Figure 38, the XRD graph shows a clear peak at 20.9°, which is the characteristic β-phase diffraction peak of crystalline PVDF. The authors explain that 100% β-phase is achieved by combined effects of the electrospinning process, polar DMF solvent, and specific interactions between the imidazolium ions of the RTIL and the CF_2 group. Figure 39 provides a schematic summarizing the relationship between the electrospinning parameters and fillers as they relate to the PVDF polymorphism.

Conclusions and Future Prospects

In this review, the current status of TIPS and electrospinning methods have been assessed, with particular focus on membrane morphology control. For the TIPS method, different parameters that affect the final membrane morphology are extensively discussed and interpreted from thermodynamic and kinetic perspectives. Also, current state-of-the-art TIPS-prepared PVDF membrane data are compiled and an upperbound (permeability vs. tensile strength) is proposed to guide future research efforts. During the preparation of this manuscript, several important trends in TIPS research were clearly visible. First, many of the TIPS studies only report on the final membrane morphology without discussing the actual membrane performance. To fully utilize the TIPS method in the membrane industry, it is necessary to prepare membranes and assess the permeability, rejection, and tensile strength. Second, research on post-treatment and additives for TIPS-prepared PVDF data are rather scarce. Such research efforts could result in a strategy to overcome the current TIPS upperbound. Last but not least, correlations between PVDF polymorphism and the overall membrane performance have not been clearly elucidated. We speculate that the surface properties of the PVDF membranes can influence the MCr performance and the fouling tendency.

With regard to the electrospinning method, the key parameters that affect the nanofiber morphology are reviewed. The unique advantage of the electrospinning method, as mentioned in the main text, is the ability to control the polymorphism phase of a semicrystalline polymer such as PVDF. Different methods to control the PVDF polymorphism (α, β, and γ-phase) are assessed. It is now possible to obtain a fully β-phase PVDF membrane using the electrospinning method. However, similar to the TIPS-prepared membranes, a specific correlation between the membrane polymorphism, surface properties, and the performance is lacking. With high porosity and uniform pore size distribution, β-phase PVDF nanofiber membranes could show interesting potential for membrane contactor applications. In particular, the effect of the surface properties on the crystallization kinetics in MCr operation is an open question.

Acknowledgments

The authors would like to thank the financial support from the Nano Material Technology Development Program (2012M3A7B4949745), the National Research Foundation of the Korean Ministry of Science, ICT and Future Planning, and also for partial support from Solvay Specialty Polymers.

Notation

ATBC = acetyl tributyl citrate
ATEC = acetyl triethyl citrate
DBP = dibutyl phthalate
DMP = dimethyl phthalate
DOA = dioctyl adipate
DOS = dioctyl sebacate
DEA = diethyl adipate
DMAc = dimethylacetamide
DBI = dibutyl itaconate
DPC = diphenyl carbonate
DMSO2 = dimethyl sulfone
DPK = diphenyl ketone
DOP = dioctyl phthalate
DEHP = di-(2-ethylhexyl) phthalate
PVA = poly(vinyl alcohol)
PEG = poly(ethylene glycol)
PMMA = poly(methyl methacrylate)
PVP = poly(vinyl pyrrolidone)
PGC = 1,2-propylene glycol carbonate
Polarclean = methyl-5-(dimethylamino)-2-methyl-5-oxopentanoate
PES-S = poly(ethersulfone)
PVDF = poly(vinylidene fluoride)
PVDF-co-HFP = poly(vinylidene fluoride-co-hexafluoropropene)
PVDF-co-TFE = poly(vinylidene fluoride-co-tetrafluoroethylene)
PVDF-co-TrFE = poly(vinylidene fluoride-co-trifluoroethylene)
PTFE = poly(tetrafluoroethylene)
ECTFE = poly(ethylene chlorotrifluoroethylene)
Hyflon AD = poly[tetrafluoroethylene-co-(2,2,4-trifluoro-5-trifluoromethoxy-1,3-dioxole)]
DEP = diethyl phthalate
DCAC = diethylene glycol monoethyl ether acetate
GTA = glycerin triacetate
GBL = γ-butyrolactone
LiCl = lithium chloride
MCr = membrane crystallization
MCr = methyl chloride
MD = membrane distillation
NMP = N-methylpyrrolidone
TEC = triethyl citrate
TEGDA = triethylene glycol diacetate
TEP = triethylphosphate
TCB = 1,3,5-trichlorobenzene
RTIL = room-temperature ionic liquid

Literature Cited

1. Elimelech M, Phillip WA. The future of seawater desalination: energy, technology, and the environment. *Science*. 2011;333(6043):712–717.
2. Van der Bruggen B, Vandecasteele C, Van Gestel T, Doyen W, Leysen R. A review of pressure-driven membrane processes in wastewater treatment and drinking water production. *Environ Prog*. 2003;22(1):46–56.
3. Charcosset C. Membrane processes in biotechnology: an overview. *Biotechnol Adv*. 2006;24(5):482–492.
4. Ciardelli G, Corsi L, Marcucci M. Membrane separation for wastewater reuse in the textile industry. *Resour Conserv Recycling*. 2001;31(2):189–197.

5. Bernardo P, Drioli E, Golemme G. Membrane gas separation: a review/state of the art. *Ind Eng Chem Res.* 2009;48(10):4638–4663.
6. Daufin G, Escudier J-P, Carrere H, Berot S, Fillaudeau L, Decloux M. Recent and emerging applications of membrane processes in the food and dairy industry. *Food Bioprod Process.* 2001;79(2):89–102.
7. Jiao B, Cassano A, Drioli E. Recent advances on membrane processes for the concentration of fruit juices: a review. *J Food Eng.* 2004;63(3):303–324.
8. Lutze P, Gorak A. Reactive and membrane-assisted distillation: recent developments and perspective. *Chem Eng Res Des.* 2013; 91(10):1978–1997.
9. Feng X, Pan CY, Ivory J, Ghosh D. Integrated membrane/adsorption process for gas separation. *Chem Eng Sci.* 1998;53(9):1689–1698.
10. Rodil R, Schrader S, Moeder M. Non-porous membrane-assisted liquid–liquid extraction of UV filter compounds from water samples. *J Chromatogr A.* 2009;1216(24):4887–4894.
11. Kuhn J, Lakerveld R, Kramer HJ, Grievink J, Jansens PJ. Characterization and dynamic optimization of membrane-assisted crystallization of adipic acid. *Ind Eng Chem Res.* 2009;48(11):5360–5369.
12. Drioli E, Stankiewicz AI, Macedonio F. Membrane engineering in process intensification—an overview. *J Membr Sci.* 2011;380(1):1–8.
13. Acmite-Market-Intelligence. *Global Membrane Technology Market*, 2013.
14. Baker RW. *Membrane Technology and Applications*. Wiley, West Sussex, United Kingdom, 2004.
15. Kim JF, Székely G, Valtcheva IB, Livingston AG. Increasing the sustainability of membrane processes through cascade approach and solvent recovery—pharmaceutical purification case study. *Green Chem.* 2014;16(1):133–145.
16. Kim JF, da Silva AMF, Valtcheva IB, Livingston AG. When the membrane is not enough: a simplified membrane cascade using Organic Solvent Nanofiltration (OSN). *Sep Purif Technol.* 2013; 116:277–286.
17. Szekely G, Jimenez-Solomon MF, Marchetti P, Kim JF, Livingston AG. Sustainability assessment of organic solvent nanofiltration: from fabrication to application. *Green Chem.* 2014;16(10):4440–4473.
18. Kim JF, Szekely G, Schaepertoens M, Valtcheva IB, Jimenez-Solomon MF, Livingston AG. In situ solvent recovery by organic solvent nanofiltration. *ACS Sustain Chem Eng.* 2014;2(10):2371–2379.
19. Smitha B, Suhanya D, Sridhar S, Ramakrishna M. Separation of organic–organic mixtures by pervaporation—a review. *J Membr Sci.* 2004;241(1):1–21.
20. Zhao C, Wang N, Wang L, Huang H, Zhang R, Yang F, Xie Y, Ji S, Li J-R. Hybrid membranes of metal-organic molecule nanocages for aromatic/aliphatic hydrocarbon separation by pervaporation. *Chem Commun.* 2014;50(90):13921–13923.
21. Adler S. *Vision 2020: 2000 separations roadmap*: Published by the Center for Waste Reduction Technologies of the AIChE in cooperation with the U.S. Dept. of Energy, Office of Industrial Technologies; 2000. 9780816908325.
22. Drioli E, Curcio E, Di Profio G. State of the art and recent progresses in membrane contactors. *Chem Eng Res Des.* 2005;83(3): 223–233.
23. Klaassen R, Feron PHM, Jansen AE. Membrane contactors in industrial applications. *Chem Eng Res Des.* 2005;83(3):234–246.
24. Klaassen R, Feron P, Jansen A. Membrane contactor applications. *Desalination.* 2008;224(1–3):81–87.
25. Drioli E, Di Profio G, Curcio E. Progress in membrane crystallization. *Curr Opin Chem Eng.* 2012;1(2):178–182.
26. Di Profio G, Curcio E, Ferraro S, Stabile C, Drioli E. Effect of supersaturation control and heterogeneous nucleation on porous membrane surfaces in the crystallization of L-glutamic acid polymorphs. *Cryst Growth Des.* 2009;9(5):2179–2186.
27. Guillen GR, Pan Y, Li M, Hoek EM. Preparation and characterization of membranes formed by nonsolvent induced phase separation: a review. *Ind Eng Chem Res.* 2011;50(7):3798–3817.
28. Lee J, Park B, Kim J, Park SB. Effect of PVP, lithium chloride, and glycerol additives on PVDF dual-layer hollow fiber membranes fabricated using simultaneous spinning of TIPS and NIPS. *Macromol Res.* 2015;23(3):291–299.
29. Hassankiadeh NT, Cui Z, Kim JH, Shin DW, Lee SY, Sanguineti A, Arcella V, Lee YM, Drioli E. Microporous poly (vinylidene fluoride) hollow fiber membranes fabricated with PolarClean as water-soluble green diluent and additives. *J Membr Sci.* 2015;479:204–212.
30. Marchetti P, Jimenez Solomon MF, Szekely G, Livingston AG. Molecular separation with organic solvent nanofiltration: a critical review. *Chem Rev.* 2014;114(21):10735–10806.
31. Cui Z, Drioli E, Lee YM. Recent progress in fluoropolymers for membranes. *Prog Polym Sci.* 2014;39(1):164–198.
32. Lee KP, Arnot TC, Mattia D. A review of reverse osmosis membrane materials for desalination—development to date and future potential. *J Membr Sci.* 2011;370(1):1–22.
33. Liu F, Hashim NA, Liu Y, Abed MM, Li K. Progress in the production and modification of PVDF membranes. *J Membr Sci.* 2011; 375(1):1–27.
34. Ameduri B. From vinylidene fluoride (VDF) to the applications of VDF-containing polymers and copolymers: recent developments and future trends. *Chem Rev.* 2009;109(12):6632–6686.
35. Salimi A, Yousefi AA. Analysis Method: FTIR studies of β-phase crystal formation *in stretched PVDF films*. *Polym Test.* 2003;22(6): 699–704.
36. Lovinger AJ. Annealing of poly(vinylidene fluoride) and formation of a fifth phase. *Macromolecules.* 1982;15(1):40–44.
37. Martins P, Lopes AC, Lanceros-Mendez S. Electroactive phases of poly(vinylidene fluoride): determination, processing and applications. *Prog Polym Sci.* 2014;39(4):683–706.
38. Correia HMG, Ramos MMD. Quantum modelling of poly(vinylidene fluoride). *Comput Mater Sci.* 2005;33(1–3):224–229.
39. Cui Z, Hassankiadeh NT, Zhuang Y, Drioli E, Lee YM. Crystalline polymorphism in poly(vinylidenefluoride) membranes. *Prog Polym Sci.* 2015. In press. doi:10.1016/j.progpolymsci.2015.07.007
40. Coster H, Farahani TD, Chilcott T. Production and characterization of piezo-electric membranes. *Desalination.* 2011;283:52–57.
41. Darestani M, Coster H, Chilcott T, Fleming S, Nagarajan V, An H. Piezoelectric membranes for separation processes: fabrication and piezoelectric properties. *J Membr Sci.* 2013;434:184–192.
42. Darestani MT, Coster HGL, Chilcott TC. Piezoelectric membranes for separation processes: operating conditions and filtration performance. *J Membr Sci.* 2013;435(0):226–232.
43. Yu S, Zheng W, Yu W, Zhang Y, Jiang Q, Zhao Z. Formation mechanism of β-phase in PVDF/CNT composite prepared by the sonication method. *Macromolecules.* 2009;42(22):8870–8874.
44. Gregorio R Jr, Cestari M. Effect of crystallization temperature on the crystalline phase content and morphology of poly (vinylidene fluoride). *J Polym Sci Part B Polym Phys.* 1994;32(5):859–870.
45. Ye Y, Jiang Y, Yu J, Wu Z, Zeng H. X-ray photoelectron spectroscopy characterization of the interface between Ag electrode and PVDF film treated by electric poling. *J Mater Sci Mater Electron.* 2006;17(12):1005–1009.
46. Ye Y, Jiang Y, Wu Z, Zeng H. Phase transitions of poly (vinylidene fluoride) under electric fields. *Integr Ferroelectr.* 2006;80(1): 245–251.
47. Venkatragavaraj E, Satish B, Vinod P, Vijaya M. Piezoelectric properties of ferroelectric PZT-polymer composites. *J Phys D Appl Phys.* 2001;34(4):487.
48. Sajkiewicz P, Wasiak A, Gocłowski Z. Phase transitions during stretching of poly(vinylidene fluoride). *Eur Polym J.* 1999;35(3): 423–429.
49. Shi L, Wang R, Cao Y, Feng C, Liang DT, Tay JH. Fabrication of poly(vinylidene fluoride-co-hexafluropropylene) (PVDF-HFP) asymmetric microporous hollow fiber membranes. *J Membr Sci.* 2007; 305(1–2):215–225.
50. Shi L, Wang R, Cao Y. Effect of the rheology of poly(vinylidene fluoride-co-hexafluropropylene) (PVDF–HFP) dope solutions on the formation of microporous hollow fibers used as membrane contactors. *J Membr Sci.* 2009;344(1–2):112–122.
51. Feng C, Shi B, Li G, Wu Y. Preparation and properties of microporous membrane from poly(vinylidene fluoride-co-tetrafluoroethylene) (F2.4) for membrane distillation. *J Membr Sci.* 2004;237(1–2):15–24.
52. He F, Sarkar M, Lau S, Fan J, Chan LH. Preparation and characterization of porous poly(vinylidene fluoride-trifluoroethylene) copolymer membranes via electrospinning and further hot pressing. *Polym Test.* 2011;30(4):436–441.
53. California A, Cardoso VF, Costa CM, Sencadas V, Botelho G, Gómez-Ribelles JL, Lanceros-Mendez S. Tailoring porous structure of ferroelectric poly(vinylidene fluoride-trifluoroethylene) by controlling solvent/polymer ratio and solvent evaporation rate. *Eur Polym J.* 2011;47(12):2442–2450.
54. Goessi M, Tervoort T, Smith P. Melt-spun poly (tetrafluoroethylene) fibers. *J Mater Sci.* 2007;42(19):7983–7990.

55. Huang Q-L, Xiao C-F, Hu X-Y, Li X-F. Study on the effects and properties of hydrophobic poly (tetrafluoroethylene) membrane. *Desalination*. 2011;277(1):187–192.
56. Bosse CF, Kowligi RR, Inventors. Uniformly Expanded PTFE Film. US patent 53211091992.
57. David N, Morizio F, Inventors. Porous polytetrafluoroethylene membrane. US patent 62740432001.
58. Takagi Y, Lee J-C, Yagi S-i, Yamane H, Wano T, Kitagawa D, El Salmawy A. Fiber making directly from poly(tetrafluoroethylene) emulsion. *Polymer*. 2011;52(18):4099–4105.
59. Ramaswamy S, Greenberg AR, Krantz WB. Fabrication of poly (ECTFE) membranes via thermally induced phase separation. *J Membr Sci*. 2002;210(1):175–180.
60. Roh IJ, Ramaswamy S, Krantz WB, Greenberg AR. Poly (ethylene chlorotrifluoroethylene) membrane formation via thermally induced phase separation (TIPS). *J Membr Sci*. 2010;362(1):211–220.
61. Müller H-JJ. A new solvent resistant membrane based on ECTFE. *Desalination*. 2006;199(1):191–192.
62. Simone S, Figoli A, Santoro S, Galiano F, Alfadul S, Al-Harbi OA, Drioli E. Preparation and characterization of ECTFE solvent resistant membranes and their application in pervaporation of toluene/water mixtures. *Sep Purif Technol*. 2012;90:147–161.
63. Gugliuzza A, Ricca F, Drioli E. Controlled pore size, thickness and surface free energy of super-hydrophobic PVDF® and Hyflon®AD membranes. *Desalination*. 2006;200(1–3):26–28.
64. Gugliuzza A, Drioli E. PVDF and HYFLON AD membranes: ideal interfaces for contactor applications. *J Membr Sci*. 2007;300(1–2):51–62.
65. Jansen JC, Tasselli F, Tocci E, Drioli E. High-flux composite perfluorinated gas separation membranes of Hyflon® AD on a hollow fibre ultrafiltration membrane support. *Desalination*. 2006;192(1–3):207–213.
66. Mulder M. *Basic Principles of Membrane Technology*: Springer Science & Business Media, Berlin, Germany; 1996. 079234247X.
67. Wang D-M, Lai J-Y. Recent advances in preparation and morphology control of polymeric membranes formed by nonsolvent induced phase separation. *Curr Opin Chem Eng*. 2013;2(2):229–237.
68. Caneba GT, Soong DS. Polymer membrane formation through the thermal-inversion process. 1. Experimental study of membrane structure formation. *Macromolecules*. 1985;18(12):2538–2545.
69. Caneba GT, Soong DS. Polymer membrane formation through the thermal-inversion process. 2. Mathematical modeling of membrane structure formation. *Macromolecules*. 1985;18(12):2545–2555.
70. Lloyd DR, Kinzer KE, Tseng H. Microporous membrane formation via thermally induced phase separation. I. Solid-liquid phase separation. *J Membr Sci*. 1990;52(3):239–261.
71. Lloyd DR, Kim SS, Kinzer KE. Microporous membrane formation via thermally-induced phase separation. II. Liquid—liquid phase separation. *J Membr Sci*. 1991;64(1):1–11.
72. Kim SS, Lloyd DR. Microporous membrane formation via thermally-induced phase separation. III. Effect of thermodynamic interactions on the structure of isotactic polypropylene membranes. *J Membr Sci*. 1991;64(1):13–29.
73. Lim GB, Kim SS, Ye Q, Wang YF, Lloyd DR. Microporous membrane formation via thermally-induced phase separation. IV. Effect of isotactic polypropylene crystallization kinetics on membrane structure. *J Membr Sci*. 1991;64(1):31–40.
74. Kim SS, Lim GB, Alwattari AA, Wang YF, Lloyd DR. Microporous membrane formation via thermally-induced phase separation. V. Effect of diluent mobility and crystallization on the structure of isotactic polypropylene membranes. *J Membr Sci*. 1991;64(1):41–53.
75. Alwattari AA, Lloyd DR. Microporous membrane formation via thermally-induced phase separation. VI. Effect of diluent morphology and relative crystallization kinetics on polypropylene membrane structure. *J Membr Sci*. 1991;64(1):55–67.
76. Lloyd DR, Lim GB. Microporous membrane formation via thermally-induced phase separation. VII. Effect of dilution, cooling rate, and nucleating agent addition on morphology. *J Membr Sci*. 1993;79(1):27–34.
77. Burghardt W. Phase diagrams for binary polymer systems exhibiting both crystallization and limited liquid-liquid miscibility. *Macromolecules*. 1989;22(5):2482–2486.
78. Hanks PL, Lloyd DR. Deterministic model for matrix solidification in liquid–liquid thermally induced phase separation. *J Membr Sci*. 2007;306(1–2):125–133.
79. Mino Y, Ishigami T, Kagawa Y, Matsuyama H. Three-dimensional phase-field simulations of membrane porous structure formation by thermally induced phase separation in polymer solutions. *J Membr Sci*. 2015;483(0):104–111.
80. He Y-D, Tang Y-H, Wang X-L. Dissipative particle dynamics simulation on the membrane formation of polymer–diluent system via thermally induced phase separation. *J Membr Sci*. 2011;368(1):78–85.
81. Li X, Lu X. Morphology of polyvinylidene fluoride and its blend in thermally induced phase separation process. *J Appl Polym Sci*. 2006;101(5):2944–2952.
82. Gu M, Zhang J, Wang X, Tao H, Ge L. Formation of poly(vinylidene fluoride) (PVDF) membranes via thermally induced phase separation. *Desalination*. 2006;192(1–3):160–167.
83. Cha BJ, Yang JM. Effect of high-temperature spinning and PVP additive on the properties of PVDF hollow fiber membranes for microfiltration. *Macromol Res*. 2006;14(6):596–602.
84. Gu M, Zhang J, Wang X, Ma W. Crystallization behavior of PVDF in PVDF-DMP system via thermally induced phase separation. *J Appl Polym Sci*. 2006;102(4):3714–3719.
85. Ji G-L, Du C-H, Zhu B-K, Xu Y-Y. Preparation of porous PVDF membrane via thermally induced phase separation with diluent mixture of DBP and DEHP. *J Appl Polym Sci*. 2007;105(3):1496–1502.
86. Su Y, Chen C, Li Y, Li J. Preparation of PVDF membranes via TIPS method: the effect of mixed diluents on membrane structure and mechanical property. *J Macromol Sci Part A Pure Appl Chem*. 2007;44(3):305–313.
87. Cui Z-Y, Xu Y-Y, Zhu L-P, Wei X-Z, Zhang C-F, Zhu B-K. Preparation of PVDF/PMMA blend microporous membranes for lithium ion batteries via thermally induced phase separation process. *Mater Lett*. 2008;62(23):3809–3811.
88. Rajabzadeh S, Maruyama T, Sotani T, Matsuyama H. Preparation of PVDF hollow fiber membrane from a ternary polymer/solvent/nonsolvent system via thermally induced phase separation (TIPS) method. *Sep Purif Technol*. 2008;63(2):415–423.
89. Gu M, Zhang J, Xia Y, Wang X. Poly (vinylidene fluoride) crystallization behavior and membrane structure formation via thermally induced phase separation with benzophenone diluent. *J Macromol Sci Part B*. 2008;47(1):180–191.
90. Yang J, Li DW, Lin YK, Wang XL, Tian F, Wang Z. Formation of a bicontinuous structure membrane of polyvinylidene fluoride in diphenyl ketone diluent via thermally induced phase separation. *J Appl Polym Sci*. 2008;110(1):341–347.
91. Li X, Xu G, Lu X, Xiao C. Effects of mixed diluent compositions on poly(vinylidene fluoride) membrane morphology in a thermally induced phase-separation process. *J Appl Polym Sci*. 2008;107(6):3630–3637.
92. Rajabzadeh S, Maruyama T, Ohmukai Y, Sotani T, Matsuyama H. Preparation of PVDF/PMMA blend hollow fiber membrane via thermally induced phase separation (TIPS) method. *Sep Purif Technol*. 2009;66(1):76–83.
93. Lu X, Li X. Preparation of polyvinylidene fluoride membrane via a thermally induced phase separation using a mixed diluent. *J Appl Polym Sci*. 2009;114(2):1213–1219.
94. Lin Y, Tang Y, Ma H, Yang J, Tian Y, Ma W, Wang X. Formation of a bicontinuous structure membrane of polyvinylidene fluoride in diphenyl carbonate diluent via thermally induced phase separation. *J Appl Polym Sci*. 2009;114(3):1523–1528.
95. Cui A, Liu Z, Xiao C, Zhang Y. Effect of micro-sized SiO 2-particle on the performance of PVDF blend membranes via TIPS. *J Membr Sci*. 2010;360(1):259–264.
96. Yang J, Wang XL, Tian Y, Lin Y, Tian F. Morphologies and crystalline forms of polyvinylidene fluoride membranes prepared in different diluents by thermally induced phase separation. *J Polym Sci Part B Polym Phys*. 2010;48(23):2468–2475.
97. Ghasem N, Al-Marzouqi M, Duaidar A. Effect of quenching temperature on the performance of poly(vinylidene fluoride) microporous hollow fiber membranes fabricated via thermally induced phase separation technique on the removal of CO2 from CO2-gas mixture. *Int J Greenhouse Gas Control*. 2011;5(6):1550–1558.
98. Rajabzadeh S, Liang C, Ohmukai Y, Maruyama T, Matsuyama H. Effect of additives on the morphology and properties of poly (vinylidene fluoride) blend hollow fiber membrane prepared by the thermally induced phase separation method. *J Membr Sci*. 2012;423:189–194.
99. Li X, Liu H, Xiao C, Ma S, Zhao X. Effect of take-up speed on polyvinylidene fluoride hollow fiber membrane in a thermally

induced phase separation process. *J Appl Polym Sci*. 2013;128(2): 1054–1060.
100. Liang H-Q, Wu Q-Y, Wan L-S, Huang X-J, Xu Z-K. Polar polymer membranes via thermally induced phase separation using a universal crystallizable diluent. *J Membr Sci*. 2013;446(0):482–491.
101. Zhang Z, Guo C, Li X, Liu G, Lv J. Effects of PVDF crystallization on polymer gelation behavior and membrane structure from PVDF/TEP system via modified TIPS process. Polym *Plast Technol Eng*. 2013;52(6):564–570.
102. Cui Z, Hassankiadeh NT, Lee SY, Lee JM, Woo KT, Sanguineti A, Arcella V, Lee YM, Drioli E. Poly(vinylidene fluoride) membrane preparation with an environmental diluent via thermally induced phase separation. *J Membr Sci*. 2013;444(0):223–236.
103. Hassankiadeh NT, Cui Z, Kim JH, Shin DW, Sanguineti A, Arcella V, Lee YM, Drioli E. PVDF hollow fiber membranes prepared from green diluent via thermally induced phase separation: effect of PVDF molecular weight. *J Membr Sci*. 2014;471(0):237–246.
104. Wu L, Sun J. Structure and properties of PVDF membrane with PES-C addition via thermally induced phase separation process. *Appl Surf Sci*. 2014;322(0):101–110.
105. Wang Z, Sun L, Wang Q, Li B, Wang S. A novel approach to fabricate interconnected sponge-like and highly permeable polyvinylidene fluoride hollow fiber membranes for direct contact membrane distillation. *Eur Polym J*. 2014;60(0):262–272.
106. Cui Z, Hassankiadeh NT, Lee SY, Woo KT, Lee JM, Sanguineti A, Arcella V, Lee YM, Drioli E. Tailoring novel fibrillar morphologies in poly(vinylidene fluoride) membranes using a low toxic triethylene glycol diacetate (TEGDA) diluent. *J Membr Sci*. 2015;473(0): 128–136.
107. Xu H-P, Lang W-Z, Zhang X, Guo Y-J. Preparation and characterizations of charged PVDF membranes via composite thermally induced phase separation (C-TIPS) method. *J Ind Eng Chem*. 2015; 21:1005–1013.
108. Wang L, Huang D, Wang X, Meng X, Lv Y, Wang X, Miao R. Preparation of PVDF membranes via the low-temperature TIPS method with diluent mixtures: the role of coagulation conditions and cooling rate. *Desalination*. 2015;361(0):25–37.
109. Sawada S-I, Ursino C, Galiano F, Simone S, Drioli E, Figoli A. Effect of citrate-based non-toxic solvents on poly(vinylidene fluoride) membrane preparation via thermally induced phase separation. *J Membr Sci*. 2015;493:232–242.
110. Drioli E, Santoro S, Simone S, Barbieri G, Brunetti A, Macedonio F, Figoli A. ECTFE membrane preparation for recovery of humidified gas streams using membrane condenser. *React Funct Polym*. 2014;79:1–7.
111. Pan J, Xiao C, Huang Q, Wang C, Liu H. Fabrication and properties of poly(ethylene chlorotrifluoroethylene) membranes via thermally induced phase separation (TIPS). *RSC Adv*. 2015;5(56): 45249–45257.
112. Tang Y-H, He Y-D, Wang X-L. Investigation on the membrane formation process of polymer–diluent system via thermally induced phase separation accompanied with mass transfer across the interface: dissipative particle dynamics simulation and its experimental verification. *J Membr Sci*. 2015;474(0):196–206.
113. Razali M, Kim JF, Attfield M, et al. Sustainable wastewater treatment and recycle in membrane manufacturing. *Green Chem*. in press. DOI:10.1039/C5GC01937K
114. Funk C, Hanks P, Kaczorowski K, Lloyd D. Diluent crystal alignment in the formation of membranes via liquid–solid thermally induced phase separation. *J Porous Mater*. 2009;16(4):453–458.
115. Gu M, Zhang J, Xia Y, Wang X. Poly (vinylidene fluoride) crystallization behavior and membrane structure formation via thermally induced phase separation with benzophenone diluent. *J Macromol Sci Part B*. 2007;47(1):180–191.
116. El Mohajir B-E, Heymans N. Changes in structural and mechanical behaviour of PVDF with processing and thermomechanical treatments. 1. Change in structure. *Polymer*. 2001;42(13):5661–5667.
117. Wang KY, Foo SW, Chung T-S. Mixed matrix PVDF hollow fiber membranes with nanoscale pores for desalination through direct contact membrane distillation. *Ind Eng Chem Res*. 2009;48(9): 4474–4483.
118. Edwie F, Teoh MM, Chung T-S. Effects of additives on dual-layer hydrophobic–hydrophilic PVDF hollow fiber membranes for membrane distillation and continuous performance. *Chem Eng Sci*. 2012;68(1):567–578.
119. Strathmann H, Kock K. The formation mechanism of phase inversion membranes. *Desalination*. 1977;21(3):241–255.
120. Strathmann H, Scheible P, Baker R. A rationale for the preparation of Loeb-Sourirajan-type cellulose acetate membranes. *J Appl Polym Sci*. 1971;15(4):811–828.
121. Altena FW, Smolders C. Calculation of liquid-liquid phase separation in a ternary system of a polymer in a mixture of a solvent and a nonsolvent. *Macromolecules*. 1982;15(6):1491–1497.
122. Bottino A, Capannelli G, Munari S, Turturro A. Solubility parameters of poly (vinylidene fluoride). *J Polym Sci Part B Polym Phys*. 1988;26(4):785–794.
123. Munari S, Bottino A, Capannelli G. Casting and performance of polyvinylidene fluoride based membranes. *J Membr Sci*. 1983;16: 181–193.
124. Cheng L-P, Young T-H, Fang L, Gau J-J. Formation of particulate microporous poly (vinylidene fluoride) membranes by isothermal immersion precipitation from the 1-octanol/dimethylformamide/poly (vinylidene fluoride) system. *Polymer*. 1999;40(9):2395–2403.
125. Cheng L-P. Effect of temperature on the formation of microporous PVDF membranes by precipitation from 1-octanol/DMF/PVDF and water/DMF/PVDF systems. *Macromolecules*. 1999;32(20):6668–6674.
126. Bottino A, Capannelli G, Munari S, Turturro A. High performance ultrafiltration membranes cast from LiCl doped solutions. *Desalination*. 1988;68(2):167–177.
127. Sukitpaneenit P, Chung T-S. Molecular elucidation of morphology and mechanical properties of PVDF hollow fiber membranes from aspects of phase inversion, crystallization and rheology. *J Membr Sci*. 2009;340(1):192–205.
128. Wienk I, Boom R, Beerlage M, Bulte A, Smolders C, Strathmann H. Recent advances in the formation of phase inversion membranes made from amorphous or semi-crystalline polymers. *J Membr Sci*. 1996;113(2):361–371.
129. Matsuyama H, Takida Y, Maki T, Teramoto M. Preparation of porous membrane by combined use of thermally induced phase separation and immersion precipitation. *Polymer*. 2002;43(19):5243–5248.
130. Cha BJ, Yang JM. Preparation of poly (vinylidene fluoride) hollow fiber membranes for microfiltration using modified TIPS process. *J Membr Sci*. 2007;291(1):191–198.
131. Xiao T, Wang P, Yang X, Cai X, Lu J. Fabrication and characterization of novel asymmetric polyvinylidene fluoride (PVDF) membranes by the nonsolvent thermally induced phase separation (NTIPS) method for membrane distillation applications. *J Membr Sci*. 2015;489:160–174.
132. Li Z, Wang C. *One-dimensional Nanostructures: Electrospinning Technique and Unique Nanofibers*. Springer, Berlin, Germany; 2013. 3642364276.
133. Rim NG, Shin CS, Shin H. Current approaches to electrospun nanofibers for tissue engineering. *Biomed Mater*. 2013;8(1):014102.
134. Wang X, Ding B, Yu J, Wang M. Engineering biomimetic superhydrophobic surfaces of electrospun nanomaterials. *Nano Today*. 2011;6(5):510–530.
135. Teo W, Ramakrishna S. A review on electrospinning design and nanofibre assemblies. *Nanotechnology*. 2006;17(14):R89.
136. Sas I, Gorga RE, Joines JA, Thoney KA. Literature review on superhydrophobic self-cleaning surfaces produced by electrospinning. *J Polym Sci Part B Polym Phys*. 2012;50(12):824–845.
137. Nuraje N, Khan WS, Lei Y, Ceylan M, Asmatulu R. Superhydrophobic electrospun nanofibers. *J Mater Chem A*. 2013;1(6):1929–1946.
138. Lin T. *Nanofibers—Production, Properties and Functional Applications*. InTech, Rijeka, Croatia; 2011.
139. Greiner A, Wendorff JH. Electrospinning: a fascinating method for the preparation of ultrathin fibers. *Angew Chem*. 2007;46(30):5670–5703.
140. Garg K, Bowlin GL. Electrospinning jets and nanofibrous structures. *Biomicrofluidics*. 2011;5(1):013403.
141. Arai T, Kawakami H. Ultrafine electrospun nanofiber created from cross-linked polyimide solution. *Polymer*. 2012;53(11):2217–2222.
142. Mit-uppatham C, Nithitanakul M, Supaphol P. Ultrafine electrospun polyamide-6 fibers: effect of solution conditions on morphology and average fiber diameter. *Macromol Chem Phys*. 2004;205(17): 2327–2338.
143. Koski A, Yim K, Shivkumar S. Effect of molecular weight on fibrous PVA produced by electrospinning. *Mater Lett*. 2004;58(3): 493–497.
144. Zhao Y, Yang Q, Lu X-F, Wang C, Wei Y. Study on correlation of morphology of electrospun products of polyacrylamide with

ultrahigh molecular weight. *J Polym Sci Part B Polym Phys.* 2005; 43(16):2190–2195.
145. McKee MG, Layman JM, Cashion MP, Long TE. Phospholipid nonwoven electrospun membranes. *Science*. 2006;311(5759):353–355.
146. Yang Q, Li Z, Hong Y, Zhao Y, Qiu S, Wang C, Wei Y. Influence of solvents on the formation of ultrathin uniform poly (vinyl pyrrolidone) nanofibers with electrospinning. *J Polym Sci Part B Polym Phys.* 2004;42(20):3721–3726.
147. Tijing LD, Choi J-S, Lee S, Kim S-H, Shon HK. Recent progress of membrane distillation using electrospun nanofibrous membrane. *J Membr Sci.* 2014;453:435–462.
148. Huang Z-M, Zhang Y-Z, Kotaki M, Ramakrishna S. A review on polymer nanofibers by electrospinning and their applications in nanocomposites. *Compos Sci Technol.* 2003;63(15):2223–2253.
149. Deitzel J, Kleinmeyer J, Hirvonen J, Tan NB. Controlled deposition of electrospun poly (ethylene oxide) fibers. *Polymer.* 2001;42(19): 8163–8170.
150. Deitzel J, Kleinmeyer J, Harris D, Tan NB. The effect of processing variables on the morphology of electrospun nanofibers and textiles. *Polymer.* 2001;42(1):261–272.
151. Yuan X, Zhang Y, Dong C, Sheng J. Morphology of ultrafine polysulfone fibers prepared by electrospinning. *Polym Int.* 2004;53(11): 1704–1710.
152. De Schoenmaker B, Van der Schueren L, Zugle R, Goethals A, Westbroek P, Kiekens P, Nyokong T, De Clerck K. Effect of the relative humidity on the fibre morphology of polyamide 4.6 and polyamide 6.9 nanofibres. *J Mater Sci.* 2013;48(4):1746–1754.
153. Casper CL, Stephens JS, Tassi NG, Chase DB, Rabolt JF. Controlling surface morphology of electrospun polystyrene fibers: effect of humidity and molecular weight in the electrospinning process. *Macromolecules.* 2004;37(2):573–578.
154. Xing C, Guan J, Li Y, Li J. Effect of a room-temperature ionic liquid on the structure and properties of electrospun poly(vinylidene fluoride) nanofibers. *ACS Appl Mater Interfaces.* 2014;6(6):4447–4457.
155. Nasir M, Matsumoto H, Danno T, Minagawa M, Irisawa T, Shioya M, Tanioka A. Control of diameter, morphology, and structure of PVDF nanofiber fabricated by electrospray deposition. *J Polym Sci Part B Polym Phys.* 2006;44(5):779–786.
156. Zheng J, He A, Li J, Han CC. Polymorphism control of poly(vinylidene fluoride) through electrospinning. *Macromol Rapid Commun.* 2007;28(22):2159–2162.
157. Ramasundaram S, Yoon S, Kim KJ, Park C. Preferential formation of electroactive crystalline phases in poly (vinylidene fluoride)/ organically modified silicate nanocomposites. *J Polym Sci Part B Polym Phys.* 2008;46(20):2173–2187.
158. Ince-Gunduz BS, Alpern R, Amare D, Crawford J, Dolan B, Jones S, Kobylarz R, Reveley M, Cebe P. Impact of nanosilicates on poly (vinylidene fluoride) crystal polymorphism: part 1. Melt-crystallization at high supercooling. *Polymer.* 2010;51(6):1485–1493.
159. Manna S, Nandi AK. Piezoelectric β polymorph in poly (vinylidene fluoride)-functionalized multiwalled carbon nanotube nanocomposite films. *J Phys Chem C.* 2007;111(40):14670–14680.
160. Kim GH, Hong SM, Seo Y. Piezoelectric properties of poly (vinylidene fluoride) and carbon nanotube blends: β-phase development. *Phys Chem Chem Phys.* 2009;11(44):10506–10512.
161. He L, Xu Q, Hua C, Song R. Effect of multi-walled carbon nanotubes on crystallization, thermal, and mechanical properties of poly (vinylidene fluoride). *Polym Compos.* 2010;31(5):921–927.
162. Nasir M, Matsumoto H, Minagawa M, Tanioka A, Danno T, Horibe H. Formation of β-Phase crystalline structure of PVDF nanofiber by electrospray deposition: additive effect of ionic fluorinated surfactant. *Polym J.* 2007;39(7):670–674.
163. Andrew J, Clarke D. Effect of electrospinning on the ferroelectric phase content of polyvinylidene difluoride fibers. *Langmuir.* 2008; 24(3):670–672.

Manuscript received Aug. 12, 2015, and revision received Sept. 22, 2015.